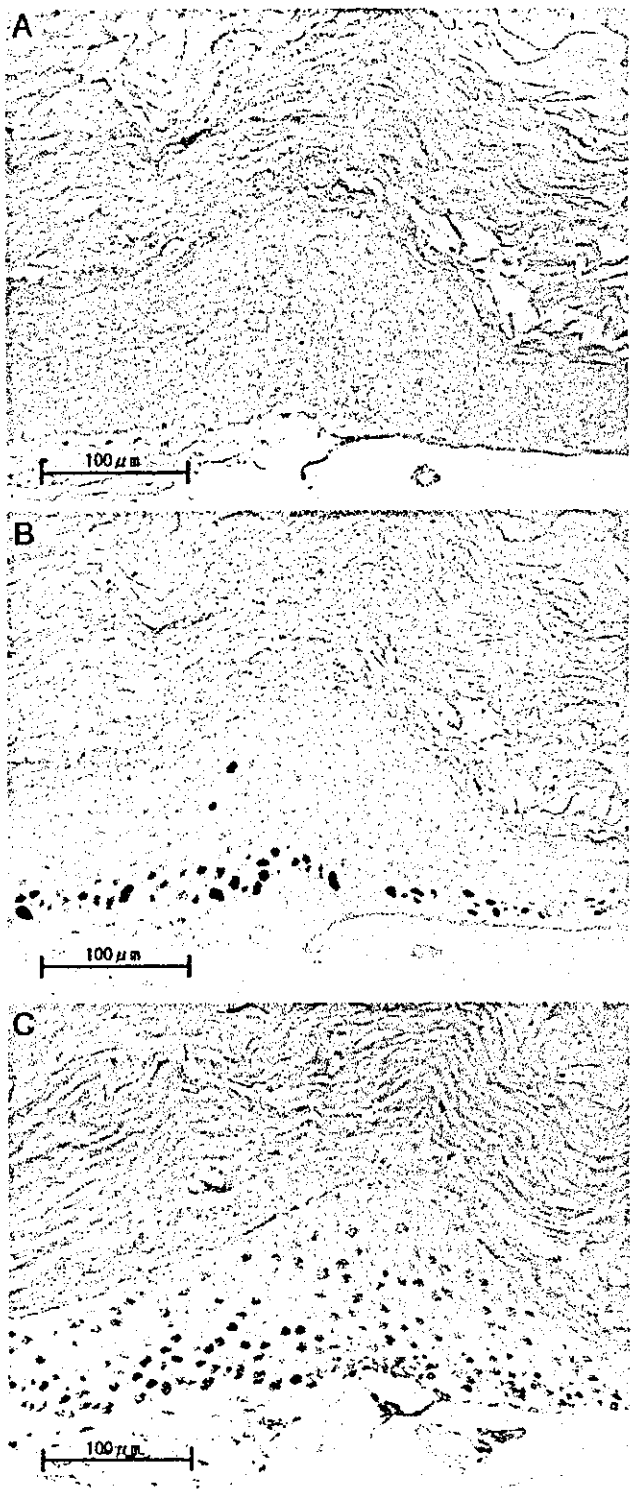

Fig. 1. Immunohistochemical staining for cholesteatoma matrix. (A) Immunohistochemical staining with anti-ErbB-2 antibody. The keratinocytes of all layers are stained as a brownish precipitate localized on the plasma membrane. (B) Immunohistochemical staining with anti-Ki-67 antibody. The nuclei of the keratinocytes of the basal, lower spinous and occasionally granular layer are stained as a brownish precipitate. (C) Immunohistochemical staining with anti-ssDNA antibody. The nuclei of the keratinocytes of al layers are stained as a brownish precipitate. (All specimens counterstained with Mayer hematoxylin; original magnification ×200.)

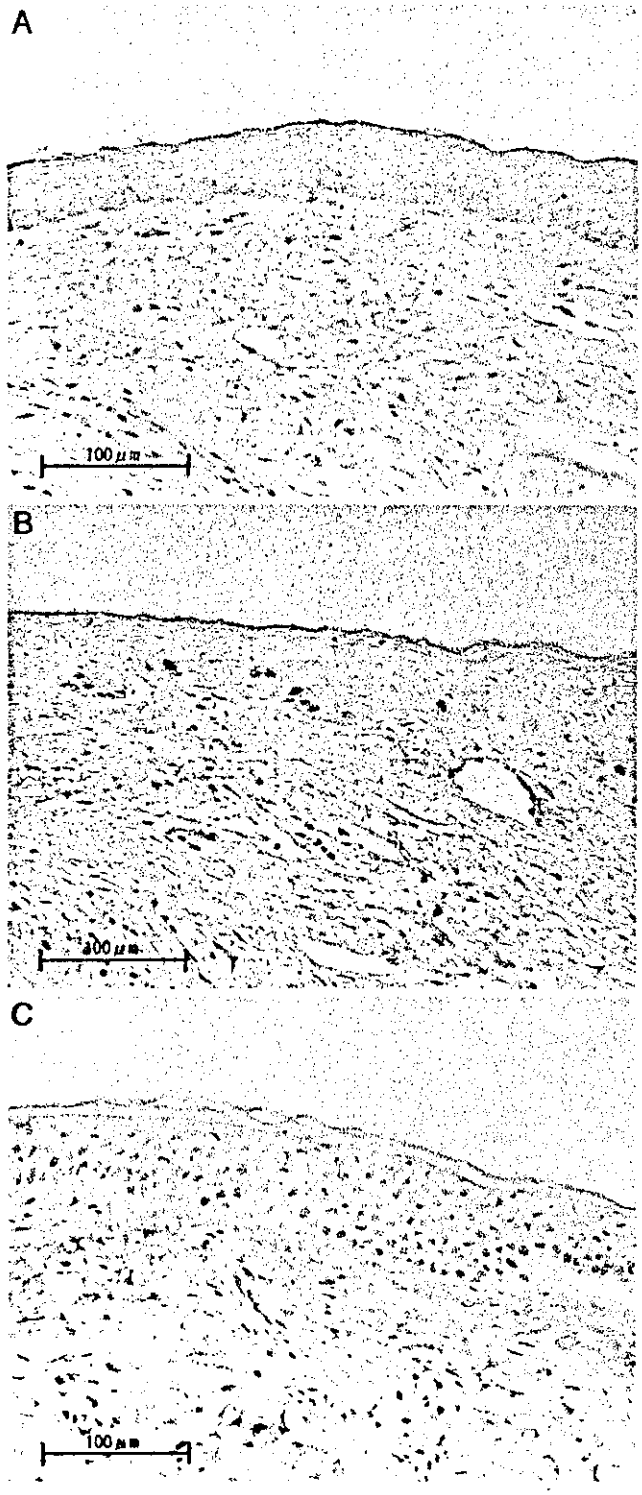

Fig. 2. Immunohistochemical staining for retroauricular skin. (A) Immunohistochemical staining with anti-ErbB-2 antibody. The keratinocytes of the basal and occasionally lower spinous layer are stained as a brownish precipitate localized in the cytoplasm in a vesicular pattern. (B) Immunohistochemical staining with anti-Ki-67 antibody. The nuclei of the keratinocytes of the basal and occasionally lower spinous layer are stained as a brownish precipitate. (C) Immunohistochemical staining with anti-ssDNA antibody. The nuclei of the keratinocytes of all layers are stained as a brownish precipitate. (All specimens counterstained with Mayer hematoxylin; original magnification ×200.)

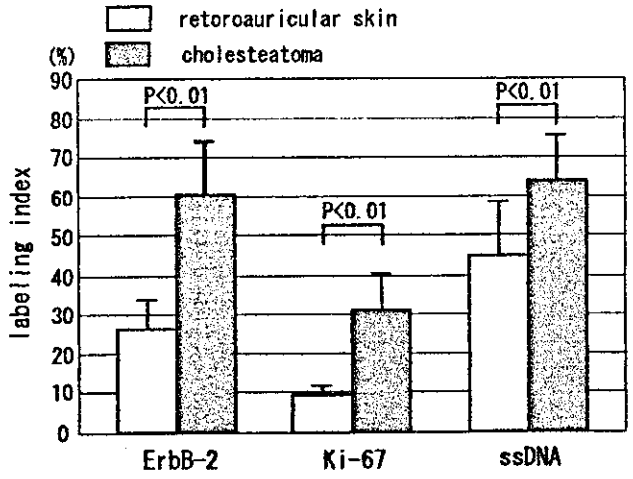

Fig. 3. Summary of the immunoreactivity of anti-ErbB-2, Ki-67, and ssDNA antibody. The labeling indices of three antibodies are compared between cholesteatoma matrix and retroauricular skin. Bars indicate standard deviations. The labeling indices of three antibodies in cholesteatoma matrix were significantly greater ($P < .01$) than those in retroauricular skin.

ated as compared with normal skin and have a greater potential of proliferation.

Single-stranded DNA modification in the nucleosomal linker region is considered a critical early step in apoptosis. A polyclonal antibody against ssDNA has been used to detect apoptotic cell death immunohistochemically in epithelial cells. In the current study, we showed the immunoreactivity of anti-ssDNA antibody in the keratinocytes of all cell layers in cholesteatoma. Although similar immunostaining pattern was observed in the retroauricular skin keratinocytes, the labeling index of anti-ssDNA antibody was significantly greater in cholesteatoma than in retroauricular skin. These findings suggest that terminal differentiation, apoptosis, is accelerated in cholesteatoma. From these findings, we could deduce the following notion that ErbB-2 protein could modulate terminal differentiation, that is, apoptosis in the keratinocytes in cholesteatoma and proliferation in the keratinocytes in retroauricular skin. Overexpression of ErbB-2 might play a crucial role in the pathogenesis of cholesteatoma by the accumulation of keratin debris as a result of enhancing apoptosis.

Although this study is a descriptive study and does not prove a mechanism to explain the difference of the effect of ErbB-2 overexpression on proliferation and apoptosis in cholesteatoma and normal skin, some speculative conclusions could be drawn from the result. It is known that keratinocytes produce cytokines[14] that induce chemotaxis of mononuclear leukocytes.[15] It can be considered that the close cell-to-cell interaction between infiltrating leukocytes and keratinocytes causes damage to the keratinocytes, and that the subsequent release of ligands of the ErbB family receptor, cytokines, and growth factors by damaged keratinocytes along with inflammatory leukocytes may change the amplification and the structure of ErbB family receptor, thus modifying control of proliferation and apoptosis in cholesteatoma.

To elucidate more exactly the role of ErbB-2 protein in the pathogenesis of human middle ear cholesteatoma, it is necessary to clarify the difference between normal skin and cholesteatoma about the coexpression pattern of the ErbB family receptor.

CONCLUSIONS

Using immunohistochemical staining, the current study demonstrated that ErbB-2 protein was overexpressed in all cell layers and that the distribution of ErbB-2 agreed with that of ssDNA in cholesteatoma matrix. We also showed that the distribution of ErbB-2 protein agreed with that of Ki-67 in retroauricular skin. These results suggest that ErbB-2 protein could modulate terminal differentiation, that is, apoptosis, in the keratinocytes of all layers in cholesteatoma and cell proliferation in the keratinocytes of the basal and occasionally lower spinous layer in normal skin.

Acknowledgments

The authors thank Ken Ito, MD, Keigo Suzukawa, MD, and Akinori Kashio, MD, Department of Otorhinolaryngology, University of Tokyo, for cooperation in obtaining surgical specimens and Yukari Kurasawa for technical advice.

BIBLIOGRAPHY

1. Klapper LN, Kirschbaum MH, Sela M, Yarden Y. Biochemical and clinical implications of the ErbB/HER signaling network of growth factor receptors. *Adv Cancer Res* 2000;77:25–79.
2. Olayioye MA, Neve RM, Lane HA, Hynes NE. The ErbB signaling network: receptor heterodimerization in development and cancer. *EMBO J* 2000;19:3159–3167.
3. Pinkas Kramarski R, Shelly M, Glathe S, Ratzkin BJ, Yarden Y. Neu differentiation factor/neuregulin isoforms activate distinct receptor combinations. *J Biol Chem* 1996;271:19029–19032.
4. Graus PD, Beerli RR, Daly JM, Hynes NE. ErbB-2, the preferred heterodimerization partner of all ErbB receptors, is a mediator of lateral signaling. *EMBO J* 1997;16:1647–1655.
5. Huang GC, Ouyang X, Epstein RJ. Proxy activation of protein ErbB2 by heterologous ligands implies a heterotetrameric mode of receptor tyrosine kinase interaction. *Biochem J* 1998;331:113–119.
6. Slamon DJ, Clark GM, Wong SG, Levin WJ, Ullrich A, McGuire WL. Human breast cancer: correlation of relapse and survival with amplification of the HER-2/neu oncogene. *Science* 1987;235:177–182.
7. Pastorino U, Andreola S, Tagliabue E, et al. Immunocytochemical markers in stage lung cancer: relevance to prognosis. *J Clin Oncol* 1997;15:2858–2865.
8. Krähn G, Leiter U, Kaskel P, et al. Coexpression patterns of EGFR, HER2, HER3 and HER4 in non-melanoma skin cancer. *Eur J Cancer* 2001;37:251–259.
9. Anu K, Alison MR, Peter CR, Yrjö TK. Studies of the inflammatory process and malignant potential of oral mucosal lichen planus. *Australian Dental J* 1996;41:87–90.
10. Henry CM, Christine J, Jeffrey AC, et al. Distribution of neu (c-erbB-2) protein in human skin. *J Invest Dermatol* 1989; 89:786–790.
11. Davina AL, Bryan Z, Steven AH, Dan FS. Inhibition of erbB receptor family members protects HaCaT keratinocytes from ultraviolet-B-induced apoptosis. *J Invest Dermatol* 2003;120:483–488.
12. Kojima H, Tanaka Y, Tanaka T, et al. Cell proliferation and apoptosis in human middle ear cholesteatoma. *Arch Otolaryngol Head Neck Surg* 1998;124:261–264.
13. Kansra S, Stoll SW, Elder JT. Differential cytoskeletal association of ErbB1 and ErbB2 during keratinocyte differentiation. *Biochem Biophys Res Commun* 2002;295:1108–1117.
14. Ansel J, Perry P, Brown J, et al. Cytokine modulation of keratinocyte cytokines. *J Invest Dermatol* 1990;94:100S–104S.
15. Yamamoto T, Osaki T, Yoneda K, Utea E. Cytokine production by keratinocytes and mononuclear infiltrates in oral lichen planus. *J Oral Pathol Med* 1994;23:309–315.

Human Molecular Genetics, 2004, Vol. 13, No. 11 *1159–1170*
DOI: 10.1093/hmg/ddh125
Advance Access published on March 31, 2004

Disruption of the *WFS1* gene in mice causes progressive β-cell loss and impaired stimulus–secretion coupling in insulin secretion

Hisamitsu Ishihara[1], Satoshi Takeda[4], Akira Tamura[1], Rui Takahashi[1], Suguru Yamaguchi[1], Daisuke Takei[1], Takahiro Yamada[1], Hiroshi Inoue[5], Hiroyuki Soga[2], Hideki Katagiri[3], Yukio Tanizawa[6] and Yoshitomo Oka[1,*]

[1]Division of Molecular Metabolism and Diabetes, [2]Division of Immunology and Embryology, and [3]Division of Advanced Therapeutics for Metabolic Diseases, Tohoku University Graduate School of Medicine, Sendai, Japan, [4]Otsuka GEN Research Institute, Otsuka Pharmaceutical Co., Tokushima, Japan, [5]Division of Diabetes and Endocrinology, Department of Medicine, Kawasaki Medical School, Kurashiki, Japan and [6]Division of Molecular Analysis of Human Disorders, Department of Bio-Signal Analysis, Yamaguchi University Graduate School of Medicine, Ube, Japan

Received February 8, 2004; Revised and Accepted March 26, 2004

Wolfram syndrome, an autosomal recessive disorder characterized by juvenile-onset diabetes mellitus and optic atrophy, is caused by mutations in the *WFS1* gene. In order to gain insight into the pathophysiology of this disease, we disrupted the *wfs1* gene in mice. The mutant mice developed glucose intolerance or overt diabetes due to insufficient insulin secretion *in vivo*. Islets isolated from mutant mice exhibited a decrease in insulin secretion in response to glucose. The defective insulin secretion was accompanied by reduced cellular calcium responses to the secretagogue. Immunohistochemical analyses with morphometry and measurement of whole-pancreas insulin content demonstrated progressive β-cell loss in mutant mice, while the α-cell, which barely expresses WFS1 protein, was preserved. Furthermore, isolated islets from mutant mice exhibited increased apoptosis, as assessed by DNA fragment formation, at high concentration of glucose or with exposure to endoplasmic reticulum-stress inducers. These results strongly suggest that WFS1 protein plays an important role in both stimulus–secretion coupling for insulin exocytosis and maintenance of β-cell mass, deterioration of which leads to impaired glucose homeostasis. These WFS1 mutant mice provide a valuable tool for understanding better the pathophysiology of Wolfram syndrome as well as WFS1 function.

INTRODUCTION

Wolfram syndrome (OMIM 222300) is a rare autosomal recessive disorder characterized by juvenile-onset non-autoimmune diabetes mellitus, optic atrophy, sensorineural deafness and diabetes insipidus (1). In addition, psychiatric illnesses such as depression and impulsive behavior are frequently observed in affected individuals (2). The nuclear gene responsible for this syndrome was identified by us (3) and others (4), and designated *WFS1* (3). More than 100 mutations of the *WFS1* gene have been identified to date in Wolfram syndrome patients. Most are inactivating mutations, suggesting loss of function to be responsible for the disease phenotype (5). WFS1 mutations underlie not only autosomal recessive Wolfram syndrome but also autosomal dominant low-frequency sensorineural hearing loss (LFSNHL). Heterozygous, non-inactivating WFS1 mutations were recently found in families with LFSNHL linked to chromosome 4p16 (DFNA6/14/38) (OMIM 600965) (6,7). The observation that the first-degree relatives of Wolfram syndrome patients have increased frequencies of diabetes mellitus and certain psychiatric disorders suggests sequence variants of the *WFS1* gene predispose these individuals to such conditions (2,8). Indeed, several WFS1 sequence variants have been shown to be significantly associated with more common forms of diabetes mellitus (9,10) as well as with suicidal and impulsive behavior (11).

*To whom correspondence should be addressed at: Division of Molecular Metabolism and Diabetes, Tohoku University Graduate School of Medicine, 2-1 Seiryo-machi, Aoba-ku, Sendai 980-8575, Japan. Tel: +81 227177173; Fax: +81 227177179; Email: oka@int3.med.tohoku.ac.jp

The WFS1 protein, also called wolframin (4), consists of 890 amino acids and was predicted to have nine or ten membrane spanning domains (3,4). Proteins with sequence similarity are now found in public databases of other organisms, *Drosophila melanogaster* (CG4917), *Anopheles gambiae* (EBIP3764) and *Fugu rubripes* (SINFRUP82345), but little is known about their functions, suggesting WFS1 protein to belong to a novel family. The WFS1 protein is expressed in various tissues but at higher levels in the brain, heart, lung and pancreas (3,4). We showed the WFS1 protein to be localized predominantly in the endoplasmic reticulum (ER) and suggested a possible role of this protein in membrane trafficking, protein processing and/or regulation of cellular calcium homeostasis (12). A recent study showed this protein to contain nine transmembrane domains and to be embedded in the ER membrane with the amino-terminus in the cytosol and the carboxy-terminus in the ER lumen (13). ER dysfunction is known to cause apoptosis, which underlies a number of genetic disorders (14,15), possibly including a subset of diabetes (15). Since severe atrophic changes have been reported in the brain and in pancreatic islets of subjects with Wolfram syndrome (16,17), it is reasonable to speculate that WFS1 protein plays an essential role in the survival of neuronal cells and islet β-cells.

In this study, to gain insight into the pathophysiology of Wolfram syndrome, we disrupted the *wfs1* gene in mice. The mice developed glucose intolerance or overt diabetes, depending on their genetic background. Our results demonstrate that the impaired glucose homeostasis in these mice results from insufficient insulin secretion due to defects in both stimulus–secretion coupling and maintenance of β-cell mass.

RESULTS

Targeted disruption of the *WFS1* gene

We first studied wfs1 protein expression in the pancreas, as this was essential to understand the diabetic phenotype in mice with a disrupted *wfs1* gene. Mouse pancreas sections were stained using an antibody raised against the 290 amino acid amino-terminus peptide of murine WFS1 (α-mWFS1-N) and those against islet hormones (Fig. 1A–L). Importantly, the WFS1 protein is strongly expressed in β-cells, and the majority of α, δ and F-cells are essentially devoid of wfs1 protein immunoreactivity. Double-staining of dispersed islet cells with these antibodies showed >80% of insulin-positive cells to be stained with anti-WFS1 antibody, while few cells express both WFS1 protein and one of the following: glucagon, somatostatin or pancreatic polypeptide (Fig. 1M–P).

In order to study the pathophysiology of Wolfram syndrome, we sought to inactivate the *wfs1* gene by inserting a neomycin-resistance gene into the second exon of the *wfs1* gene which contains the initial ATG codon (Fig. 2A and B). When analyzed using an antibody against α-mWFS1-N, WFS1 protein bands of 95 kDa were abolished in whole-brain lysates from mutant mice (Fig. 2C). In addition, WFS1 protein staining was detected in neither pancreatic islets (Fig. 2D and E) nor the hippocampus (Fig. 2F and G) in mutant animals. It was subsequently recognized that our disruption strategy resulted in altered splicing transcripts in mutant animals. Reverse transcription–polymerase chain reaction on brain, heart and islet mRNA revealed existence of a *wfs1* mRNA that lacks exon 2 in mutant animals (data not shown). Such an altered mRNA was not detected in wild-type tissues. The mutant transcript could generate amino-terminus-truncated WFS1 protein resulting from initiation of translation from one of the internal methionines. There exist methionine residues at 81, 184, 230 and 299, as well as further downstream, in murine WFS1 protein. We constructed a cDNA encoding WFS1 protein lacking the first 80 amino acids (WFS1-del80) and expressed it in COS7 cells. The WFS1-del80 protein was recognized by the antibody α-mWFS1-N (data not shown), while no bands were detected in brain lysates from mutant animals (Fig. 2C), indicating that WFS1-del80 is not expressed in mutant mice and that mutant proteins, if present, would be WFS1 protein lacking the first 183 amino acids or with larger truncations. We speculate that such truncated WFS1 proteins do not have normal functions since human substitution mutations at alanine 126, alanine 133 or glutamate 169 and a deletion mutation that lacks both lysine 178 and alanine 179 residues cause Wolfram syndrome (5). Therefore, we conclude that WFS1 function is lost, or at least severely impaired, in mice with a disrupted *wfs1* gene.

Mice homozygous for the mutated *wfs1* gene constitute the expected 25% of offspring born to heterozygous mutant parents, and are normal in appearance, growth and fertility. We did not see ataxic posture or gait disturbance. In addition, there were no differences in urine osmolality between wild-type and mutant mice. In the following experiments only male mice were used because an earlier study indicated females to have a milder phenotype. Since juvenile-onset diabetes mellitus is the most prominent feature of Wolfram syndrome, we have focused on this issue herein. Detailed studies on other aspects of this syndrome, including optic atrophy, hearing disorders, diabetes insipidus or psychiatric illness, are currently underway.

Impaired glucose homeostasis in mutant mice

Blood glucose levels in these mice were studied in non-fasted states. Initially, using mice on the [(129Sv × B6) × B6]F2 hybrid background, we found that blood glucose levels of mutant mice started to rise at around 16 weeks of age and >60% of mice (8 out of 13) had overt diabetes by 36 weeks (Fig. 3A). Since the heterogeneous contribution of B6 and 129Sv strains in the mixed background mice could cause a large variance in data, making interpretation difficult, we sought to generate mutant animals on a nearly homogenous genetic background. For this purpose, male mice with a disrupted *wfs1* gene were backcrossed for five successive generations with female mice of the B6 strain, which is frequently used for diabetes and obesity research. On the B6 background, no apparent increase in blood glucose levels was observed even at 36 weeks in mice homozygous for disrupted *wfs1* alleles (Fig. 3B). However, impaired glucose homeostasis was evident in mice on the B6 background when they were subjected to oral glucose tolerance test (Fig. 3C). Blood glucose levels at 15 and 30 min were significantly higher in mutant than in wild-type mice at 17 weeks of

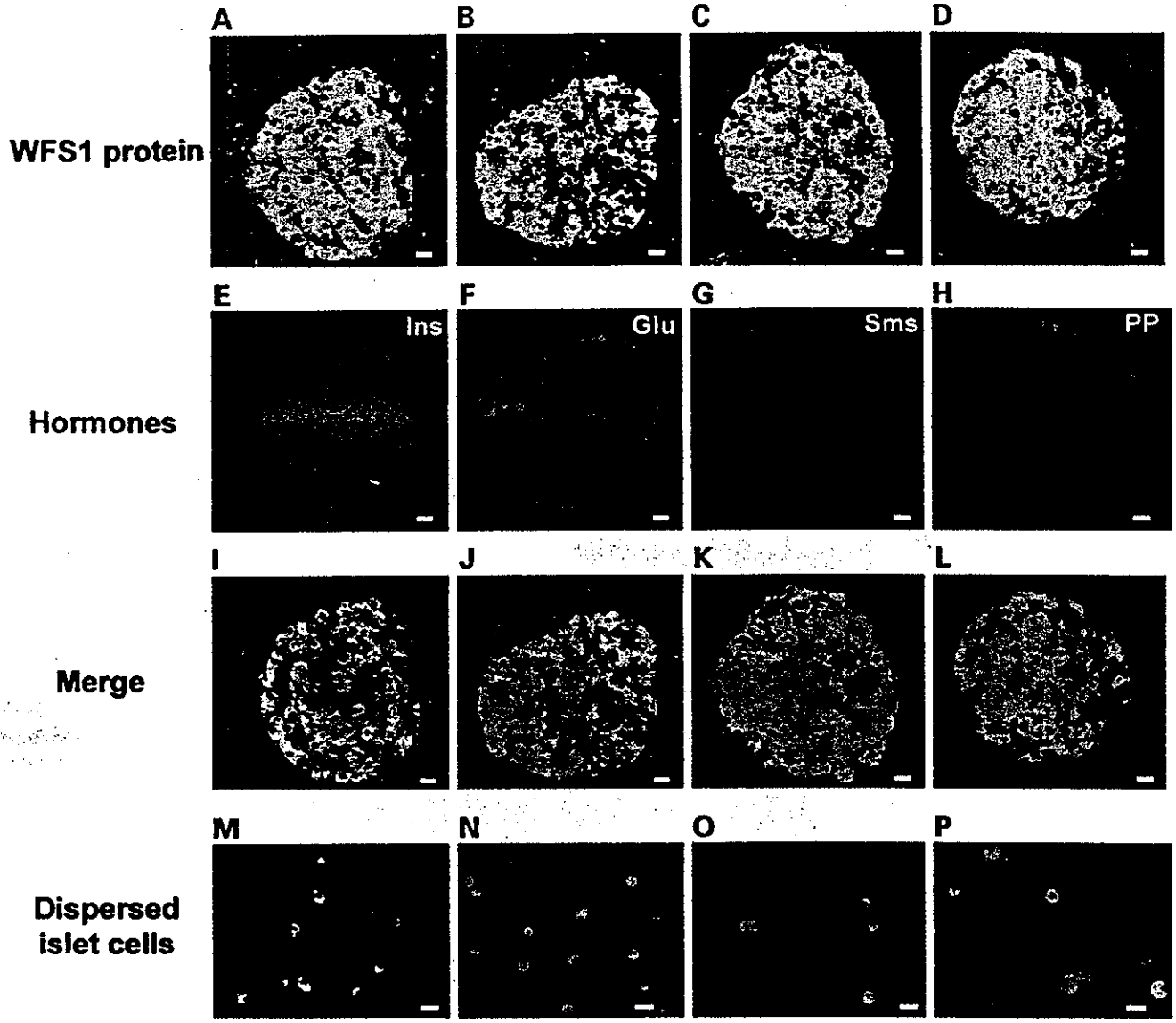

Figure 1. β-Cell specific expression of WFS1 protein in the pancreas. (A–L) Paraffin embedded mouse pancreatic sections were immunostained with antibodies against WFS1 protein (green) (A–D) and islet hormones (red): insulin (E), glucagon (F), somatostatin (G), or pancreatic polypeptide (H). A and E are the same section, and the two are merged in I. Similarly, J, K, L are merged versions of B and F, C and G, D and H, respectively. Bars = 10 μm. Ins, insulin; Glu, glucagon; Sms, somatostatin; PP, pancreatic polypeptide. (M–P) Dispersed islet cells were stained with anti-WFS1 antibody (green) together with those against islet hormones (red): insulin (M), glucagon (N), somatostatin (O) or pancreatic polypeptide (P). Bars = 10 μm.

age. These data indicated that disruption of the *wfs1* locus induced impaired glucose homeostasis in mice, as is seen in human Wolfram syndrome.

In order to investigate the pathophysiology of impaired glucose homeostasis in mutant mice, plasma immunoreactive insulin (IRI) levels in response to a glucose load were evaluated. Although plasma insulin levels after a 6 h fast were comparable between wild-type and mutant animals at 17 weeks of age (Fig. 3D), hormone responses were markedly blunted in WFS1-deficient mice. We also studied non-fasting plasma insulin levels in these mice. Plasma insulin levels in mutant mice were similar to that in wild-type mice at 24 weeks but had decreased to half the wild-type level at 36 weeks (Fig. 3E). Intraperitoneal insulin injection tests did not show insulin resistance in mutant mice at 14 (data not shown) and 19 weeks (Fig. 3F). In fact, WFS1-deficient mice were somewhat more insulin sensitive. Taken together, these data indicate impaired glucose homeostasis in mice with a disrupted *wfs1* gene to be due to insulin secretory defects rather than insulin resistance.

Impaired stimulus–secretion coupling in β-cells from mutant mice

Since defects in both stimulus–secretion coupling and insulin production could be the cause of insulin secretory defects *in vivo*, insulin secretory responses were studied using isolated islets. When we isolated islets from these mice, we noticed that

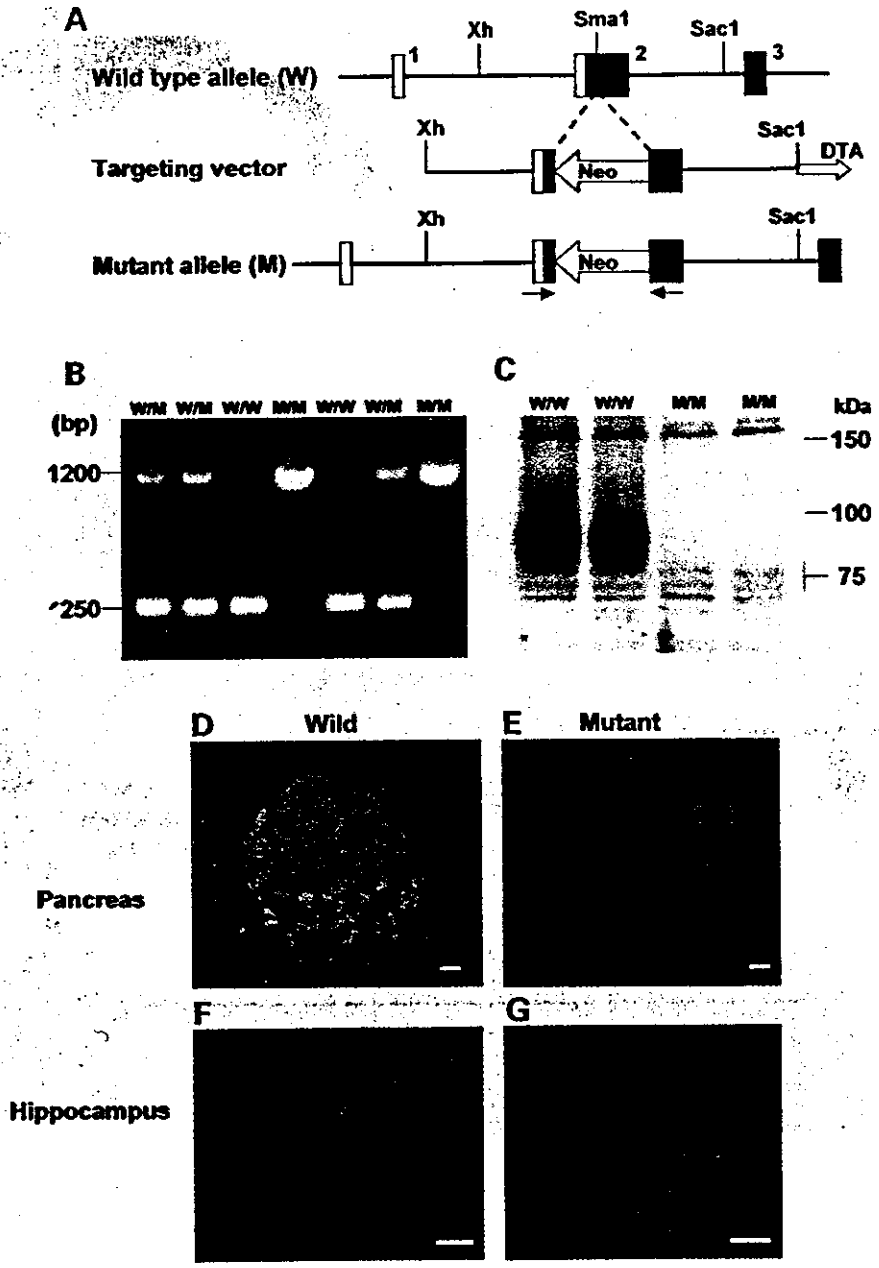

Figure 2. Targeted disruption of the *WFS1* gene. (A) Schematic representation of the mouse *wfs1* targeting strategy. Boxes are exons. Neo, neomycin resistance gene; DTA, diphtheria toxin A chain gene. (B) PCR genotyping of mutant mice. A 1200 bp longer band is observed in DNA from the disrupted allele. (C) Western blot analysis using whole-brain lysates from wild-type and mutant animals probed with anti-WFS1 antibody. (D–G) Immunohistochemical analyses using anti-WFS1 antibody in pancreatic (D, E) and hippocampal (F, G) tissues from 14-week-old wild-type and mutant mice. Bars = 10 μm for pancreatic sections and 50 μm for hippocampal sections.

it was possible to obtain only 100 islets or even less from a mutant mouse, while around 200 islets can normally be isolated from a wild-type mouse. Insulin content in the WFS1-deficient islets was slightly (16%) but significantly less than that in islets of wild-type mice [61.8 ± 2.3 ng/islet ($n = 10$ experiments) versus 73.4 ± 3.3 ($n = 10$ experiments), $P = 0.039$, mutant and wild-type islets, respectively]. We used these islets infected with either AdCAGlacZ (as a control) or AdCAGmWFS1 (Fig. 4A), because we also wanted to examine effects of WFS1 re-expression in WFS1-deficient islets and of its overexpression in wild-type islets. Glucose (15 mM)-stimulated insulin secretion, after normalization with insulin content, was reduced by 23% in islets from mutant mice (Fig. 4B). Carbachol (1.0 mM)-stimulated insulin secretion, which is thought to be evoked by Ca^{2+} release from the ER and Ca^{2+} entry through the Ca^{2+} release-activated channel, was also reduced by 26% (Fig. 4C). When WFS1 protein was re-expressed in islets from mutant animals via a recombinant adenovirus,

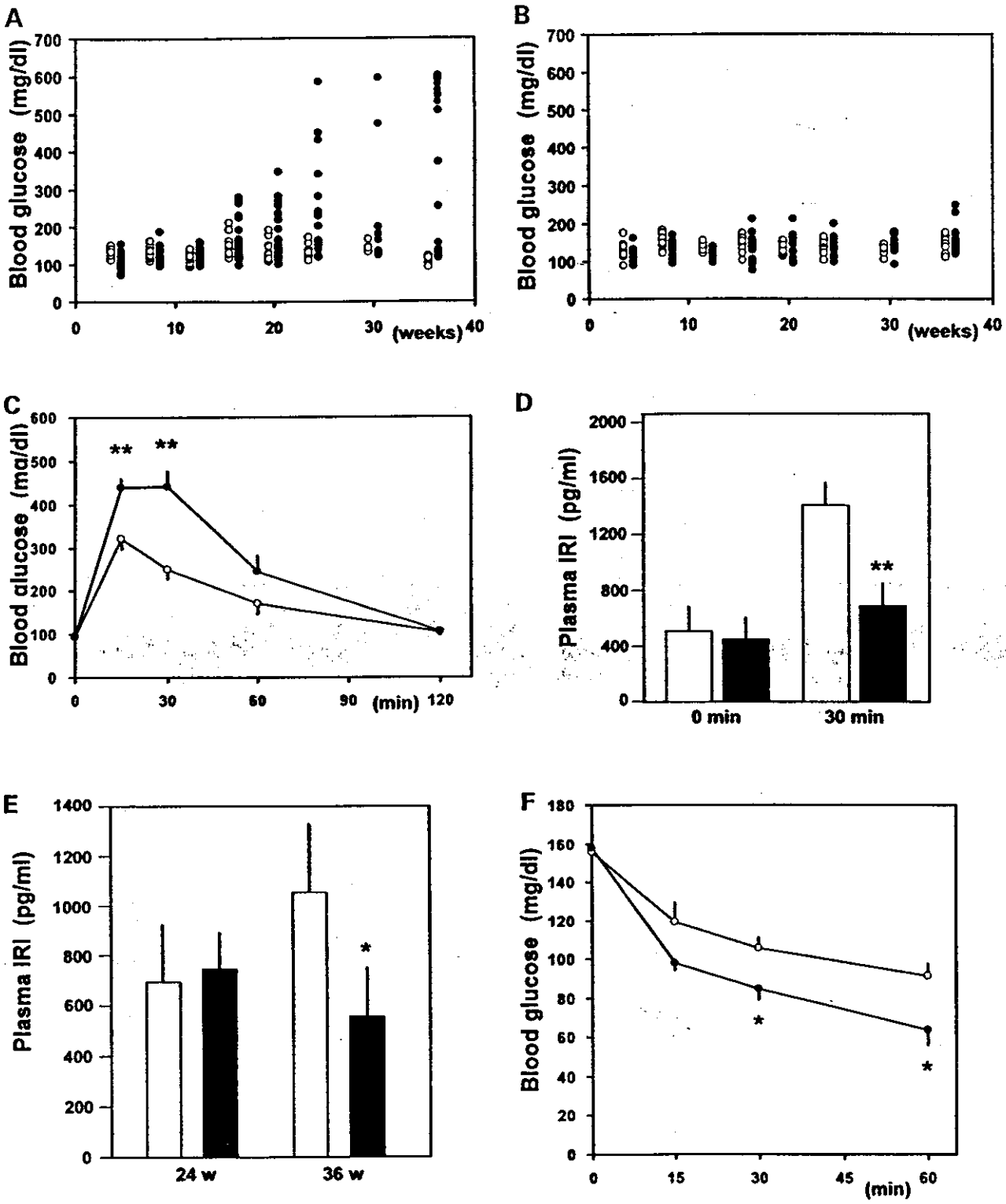

Figure 3. Impaired glucose homeostasis in WFS1-deficient mice. (**A**) Non-fasted blood glucose levels in male mice on the [(129Sv × B6) × B6]F2 hybrid background at indicated ages ($n = 8–13$). (**B**) Non-fasted blood glucose levels in male mice on the B6 background ($n = 9–16$). (**C, D**) Oral glucose (2 mg/g body weight) tolerance test in 17-week-old mice on the B6 background ($n = 6$). Blood glucose levels (C) at indicated points and plasma IRI levels (D) before and 30 min after the glucose load are shown. Glucose tolerance tests were performed on two other occasions using different animals with essentially same results. (**E**) Plasma IRI levels at 24 and 36 weeks of age ($n = 6–8$). (**F**) Insulin (0.75 units/kg body weight) tolerance test at 19 weeks ($n = 5$). Insulin tolerance tests were performed on two other occasions with essentially same results. White circles and bars, wild-type mice; black circles and bars, mutant mice. $^{*}P < 0.05$, $^{**}P < 0.01$.

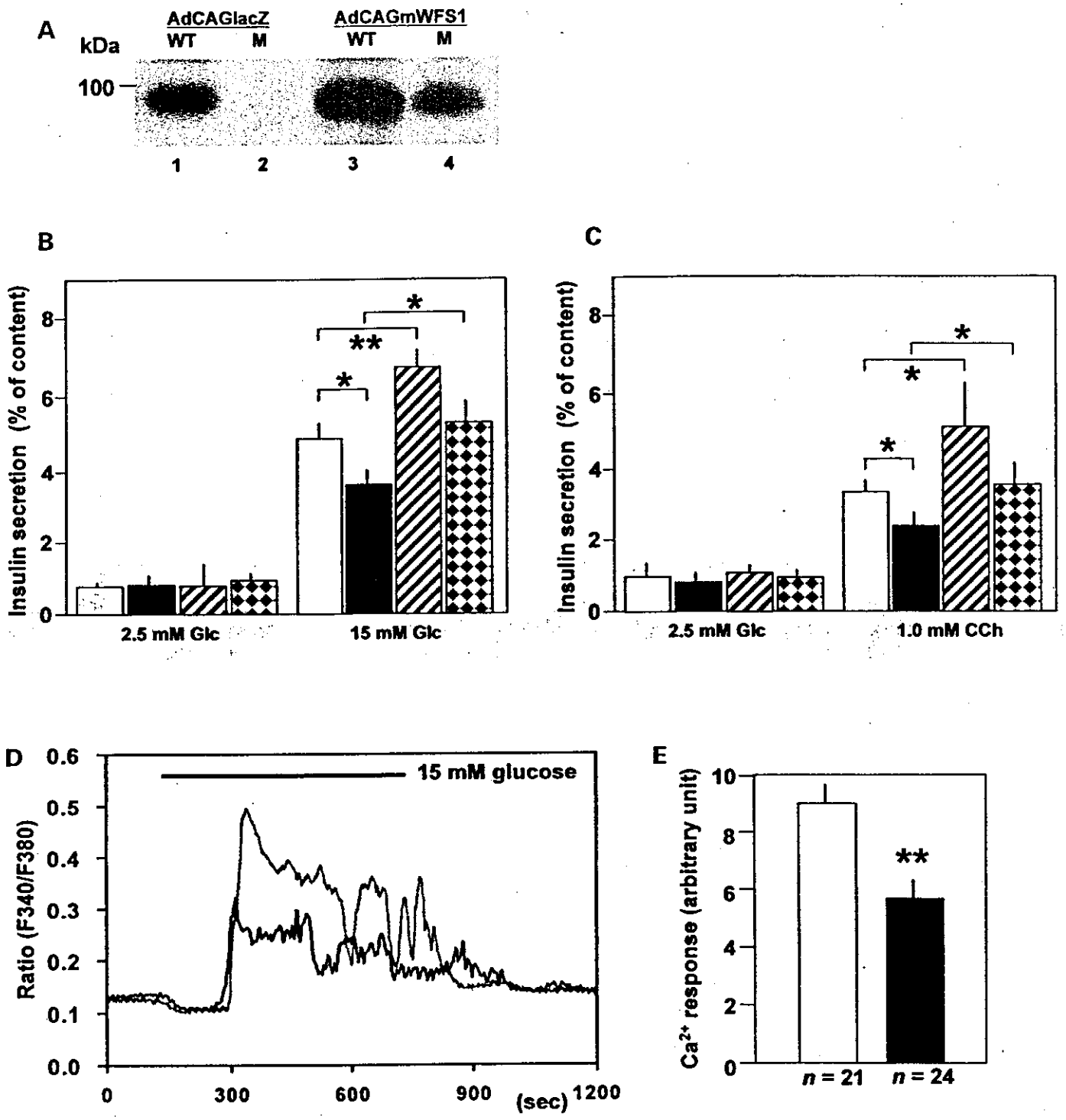

Figure 4. Impaired stimulus–secretion coupling in WFS1-deficient β-cells. (A) Islets from wild-type and mutant mice were infected with either AdCAGlacZ or AdCAGmWFS1. After 36 h, islets were subjected to western blot analyses using anti-WFS1 antibody. Lane 1, wild-type islets infected with AdCAGlacZ; lane 2, mutant islets infected with AdCAGlacZ; lane 3, wild-type islets infected with AdCAGmWFS1; lane 4, mutant islets infected with AdCAGmWFS1. Western blot experiments were performed twice with similar results and one of them is shown. (B, C) Islets were challenged with 15 mM glucose (B) or 1 mM carbachol in the presence of 2.5 mM glucose (C) for 1 h. Absolute insulin secretion in response to glucose was 3.11 ± 0.34 and 2.03 ± 0.26 ng/islet/h, respectively, for wild-type and mutant islets infected with the control virus (AdCAGlacZ). Data are means ± SEM, $n = 5$ experiments. White bars, wild-type islets infected with AdCA-lacZ; black bars, mutant islets with AdCAGlacZ; hatched bars, wild-type islets with AdCAGmWFS1; dotted bars, mutant islets with AdCAGmWFS1. (D, E) Intracellular Ca^{2+} responses to 15 mM glucose in wild-type (gray line and white bar) and WFS1-deficient (black line and black bar) β-cells. Representative traces out of 21 wild-type and 24 WFS1-deficient β-cells from one experiment were shown in D. Areas under the curve during a 5 min period after the onset of Ca^{2+} rises to glucose were summarized in E. Similar significant differences were observed in the other four experiments. $^{*}P < 0.05$, $^{**}P < 0.01$.

glucose- and carbachol-stimulated insulin secretion was restored (Fig. 4B and C), indicating reduced insulin secretion in islets from mutant mice to be a direct consequence of absence of normal WFS1 function. Interestingly, glucose- and carbachol-stimulated insulin secretion from wild-type islets increased by 41 and 53%, respectively, with overexpression of the WFS1 protein, suggesting involvement of the WFS1 protein in stimulus–secretion coupling for insulin exocytosis (Fig. 4B and C).

To gain insight into the mechanisms of impaired insulin secretion in islets from mutant mice, intracellular calcium dynamics were then studied in single β-cells challenged with glucose. The glucose-stimulated rise in the cytosolic Ca^{2+} response was reduced by 36% in WFS1-deficient β-cells when compared with that in wild-type β-cells (Fig. 4D and E).

Progressive β-cell loss in mutant mice

We then focused on aspects of insulin production, deterioration of which could be a cause of impaired glucose homeostasis in mice with disruption of the *wfs1* gene. There were no differences in pancreatic weight between wild-type and mutant mice (data not shown). Whole-pancreas insulin content was already decreased at 2 weeks, the earliest age studied, and dropped further with age (Fig. 5A). Immunohistochemical studies (Fig. 5B–E) showed the number of insulin-positive cells to be reduced at 36 weeks in the mutant mouse pancreas (Fig. 5E). Morphometric analysis demonstrated a marked reduction in the insulin-positive area per pancreatic area in mutant mice when compared with wild-type mice (Fig. 5H), indicating the decrease in insulin content to be due to loss of islet β-cells. These features were more prominent in the mutant mouse pancreas on the [(129Sv × B6) × B6]F2 background, which was associated with overt diabetes (Fig. 5F and G). In contrast to the β-cell changes, glucagon-positive cells were increased and scattered throughout WFS1-deficient islets (Fig. 5E and G). Indeed, the pancreatic glucagon content in mutant mice at 36 weeks of age on the B6 background was 2.4-fold higher than that in wild-type mice [12.3 ± 1.8 ng/mg ($n = 4$) versus 5.2 ± 0.7 ($n = 4$), $P = 0.0296$].

Increased susceptibility of WFS1-deficient islets to apoptosis

To study whether the observed β-cell loss was due to increased apoptosis, we conducted an extensive search for apoptotic β-cells in pancreatic sections. However, TUNEL or activated-caspase 3-positive cells were sparse within islets in pancreatic sections from both mutant and wild-type animals (data not shown). Therefore, we turned to *in vitro* studies, and examined whether WFS1-deficient islet cells are more susceptible to apoptotic insults. For this purpose, apoptotic DNA fragmentation was studied in isolated islets by the ligation-mediated PCR (LM-PCR) method. When islets were cultured for 3 days in RPMI media with 5 or 25 mM glucose, ladder formation was increased at 25 mM glucose in both wild-type and mutant islets when compared with that at 5 mM glucose, indicating that apoptotic cell death may have been induced by glucose toxicity (Fig. 6A). Importantly, at 25 mM glucose, islets from mutant mice showed more DNA fragment formation than wild-type islets (1.7 ± 0.3-fold, $n = 5$), while no significant differences were observed at 5 mM glucose. Since recent studies have suggested so-called ER-stress to be an important mediator of apoptosis in β-cells (14,15), DNA fragmentation was studied after treatment with two different ER-stress inducers (18), tunicamycin (2 μg/ml) and thapsigargin (2 μM). DNA fragmentation at 5 mM glucose was significantly increased, by 2.2 ± 0.4-fold and 2.4 ± 0.4-fold after tunicamycin (Fig. 6B) and thapsigargin (Fig. 6C) treatments, respectively, in WFS1-deficient islets when compared with wild-type islets. In contrast, there were no differences in DNA fragmentation after combined tumor necrosis factor-α and interferon-γ treatment (Fig. 6D), which triggers apoptosis through a signaling pathway different from that originating in the ER.

DISCUSSION

We generated mice with a disrupted *wfs1* gene. Although the diabetic phenotype was milder than that seen clinically in Wolfram syndrome (1), the progressive β-cell loss and impaired glucose homeostasis observed in these mice are essentially consistent with findings in patients (1,17). Thus, the mutant mice are indeed a model of Wolfram syndrome. The underlying anatomic condition of this syndrome has not been studied in great detail in humans, and the cellular basis for the diabetic phenotype and associated neuro-psychiatric disorders remains obscure. Creation of an animal model that reflects aspects of the disease is thus an important first step in understanding Wolfram syndrome.

The present data demonstrate that the pathophysiological basis of diabetes in Wolfram syndrome is insufficient insulin secretion due to progressive β-cell loss and impaired stimulus–secretion coupling in β-cells. Progressive β-cell loss has been expected from clinical observations of progressive deterioration of insulin-requiring states in affected patients as well as their postmortem findings, i.e. selective β-cell loss with an increase in α-cells and preservation of δ-cells (17). In contrast, impaired stimulus–secretion coupling in the β-cell, a quite unexpected result, was demonstrated for the first time in this study. In addition, we also showed for the first time that WFS1 protein is expressed selectively in β-cells, but very little in α, δ and F-cells, within the endocrine pancreas, suggesting that β-cell loss is a direct consequence of WFS1 deficiency.

The severity of the diabetic phenotype due to *wfs1* gene disruption was dependent on the mouse genetic background: >60% of mice on the [(129Sv × B6) × B6]F2 background developed overt diabetes, while mutant mice on the B6 background had impaired glucose tolerance but not overt diabetes. Modifying effects of genetic background on glucose homeostasis have been reported previously in a number of mutant mice. An earlier pioneering study established that the B6 background confers more diabetes resistance to db/db and ob/ob mice (19). A diabetes-resistant phenotype has also been reported in insulin receptor substrate (IRS)-2 knockout mice on the B6 background (20), while anti-sense glucokinase-mRNA expressing mice (21) and mice double heterozygous for deletion of the insulin receptor and IRS-1 (22), on the same B6 background, were reportedly diabetes prone. Therefore, the

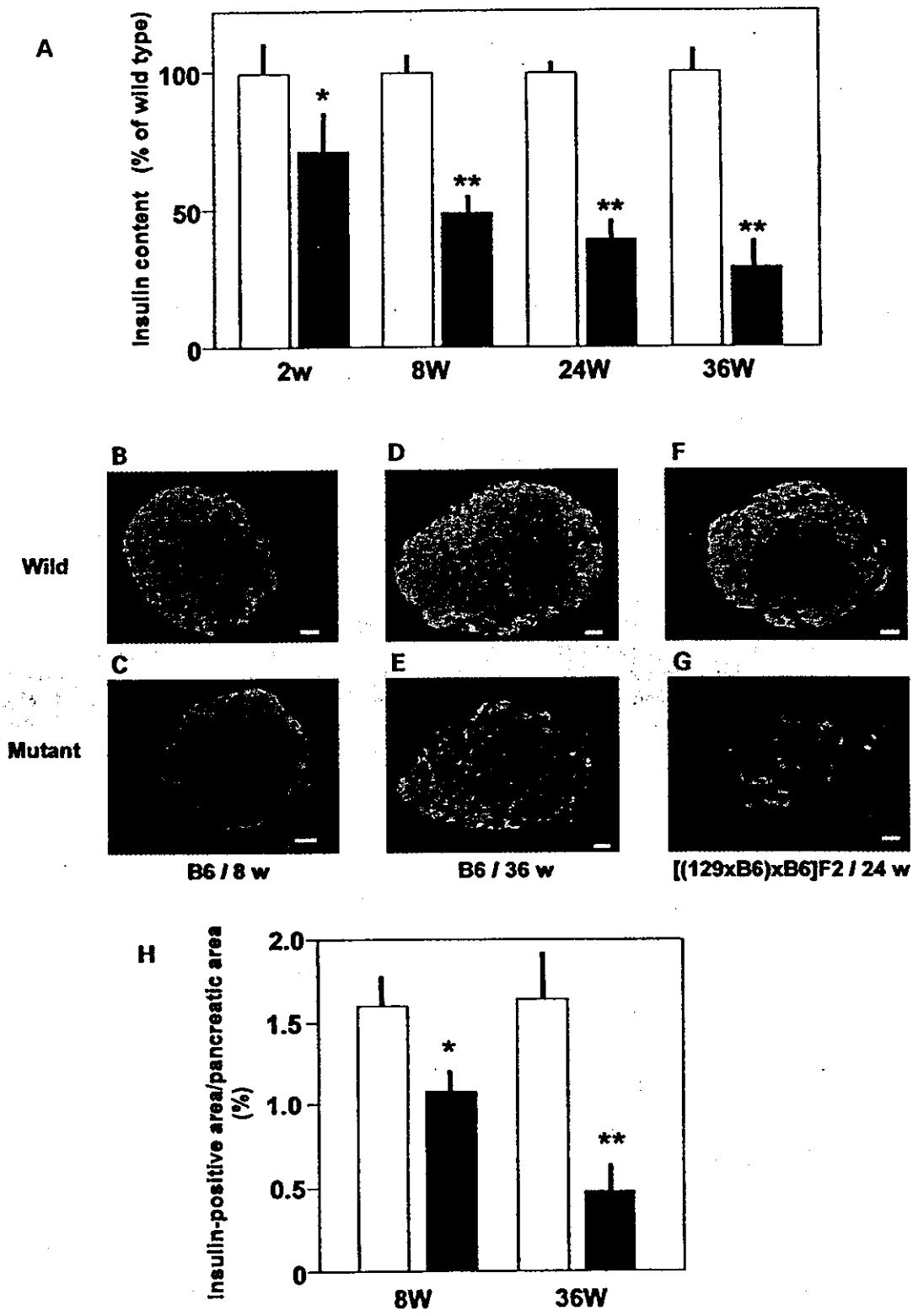

Figure 5. Progressive β-cell loss in mutant mice. (A) Insulin content extracted from whole pancreata of wild-type and mutant mice. Data represent percent of insulin content in wild-type littermates. Absolute insulin content in wild-type pancreata were 1367 ± 103 ng/mg pancreas at 2 weeks, 268 ± 18 (8 weeks), 329 ± 25 (24 weeks) and 372 ± 33 (36 weeks), $n = 4-7$. White bars, wild-type pancreata; black bars, WFS1-deficient pancreata. (B–G) Insulin (green) and glucagon (red) are stained in pancreatic sections from 8-week-old wild-type (B), mutant (C), 36-week-old wild-type (D) and mutant mice (E) on the B6 background, and 24-week-old wild-type (F) and mutant (G) mice on the [(129Sv × B6) × B6]F2 background. Bars = 10 μm. (H) Ratios of total insulin-positive area per whole pancreatic area in pancreas from wild-type and mutant mice on the B6 background. $n = 4$ animals for each group. $^{*}P < 0.05$, $^{**}P < 0.01$.

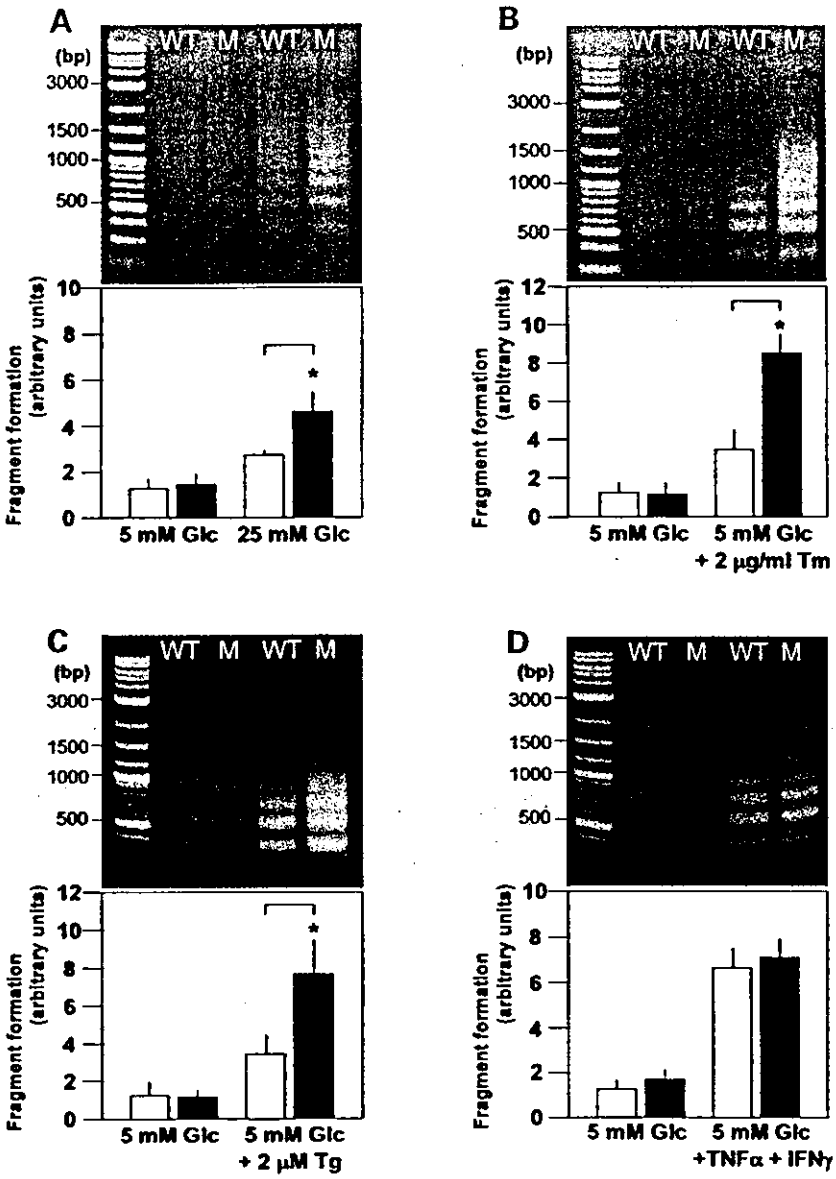

Figure 6. Increased apoptosis susceptibility in islets from mutant mice. (A) Islets from wild-type and mutant mice were cultured for 3 days in 5 and 25 mM glucose concentrations and DNA fragmentation was assessed by the LM-PCR method. (B–D) Islets from wild-type and mutant mice were treated with tunicamycin (Tm; 2 μg/ml) (B), thapsigargin (Tg; 2 μM) (C) for 24 h or with the combination of tumor necrosis factor-α (TNFα; 500 units/ml) and interferon-γ (IFNγ; 100 units/ml) (D) for 48 h and DNA fragmentation was assessed by the LM-PCR method; $n = 4–6$ experiments. $^*P < 0.05$.

contribution of genetic background is apparently complex. In any case, progressive β-cell loss was observed in mutant mice in both [(129Sv × B6) × B6]F2 and B6 strains, independent of the mouse genetic background. It is not surprising that mutant mice on the B6 background did not develop overt diabetes. Overt diabetes was known to be induced when >90% of the pancreas was removed (23), while the insulin content of mutant mouse pancreas at 36 weeks was decreased by 73% on the B6 background in this study.

The present data provide an intriguing clue that may help to elucidate WFS1 protein function. WFS1-deficient islets exhibited impaired insulin secretion in response to glucose and carbachol, which was restored by re-expression of WFS1 protein. In addition, overexpression of WFS1 protein in wild-type islets resulted in an increase in glucose- and carbachol-induced insulin secretion. These data from islets with different WFS1 protein levels demonstrated this protein to be involved directly in the regulation of insulin secretion. Furthermore, impaired calcium responses to glucose suggested that WFS1 protein is involved in regulation of calcium homeostasis in the β-cell. This notion is supported by the recent report that expression of WFS1 protein in *Xenopus* oocytes confers a novel cation channel activity (24). The present data also provide insight into the mechanism of β-cell loss in mice with a mutant *wfs1* gene. Although we rarely detected apoptotic cells in pancreatic sections from mutant mice, apoptosis cannot be excluded as a possible mechanism of β-cell loss, since our failure could presumably be due to slow progression of apoptosis *in vivo*

and rapid clearance of cells undergoing apoptosis, as was suggested recently in another animal model of diabetes (25). Increased apoptosis susceptibility in response to high glucose and ER-stress inducers, demonstrated in isolated islets from mutant mice, is likely to contribute to β-cell loss. In contrast, the apoptosis induced by exposure to tumor necrosis factor-α and interferon-γ, in which the ER-stress response is not involved, did not differ between wild-type and WFS1-deficient islets. Although the mechanism whereby high concentrations of glucose induce apoptosis is not completely understood at present (26,27), increased insulin translation in *perk*$^{-/-}$ islets indicates the ER-stress response or the unfolded protein response to be operative in islets cultured with high concentrations of glucose (28). Therefore, it is possible that increased DNA fragmentation in WFS1-deficient islets at 25 mM glucose could also be attributable to increased susceptibility to ER-stress-induced apoptosis. However, it remains to be clarified how WFS1 deficiency renders β-cells more susceptible to apoptosis, especially to ER-stress-induced apoptosis.

Recent studies showing β-cell mass to be decreased in human type 2 diabetes, due to increased β-cell apoptosis (29), have attracted considerable attention to this potential pathogenic mechanism of type 2 diabetes development. Therefore, maintaining β-cell mass is an important strategy for preventing diabetes as well as halting disease progression. Since the WFS1 protein is likely to belong to a novel family, elucidating the WFS1 protein function could lead to establishment of new treatments not only for Wolfram syndrome but also for more common forms of diabetes mellitus.

MATERIALS AND METHODS

Targeted disruption of the *wfs1* gene

The *wfs1* gene was cloned from a 129Sv mouse genomic DNA library using its cDNA probe (3). A targeting vector was constructed by inserting a neomycin-resistance gene at the *Sma*I site in exon 2 of the *wfs1* gene. The diphtheria toxin A chain expressing unit was inserted downstream (Fig. 2A). The *wfs1* gene targeting vector was microinjected into 129Sv embryonic stem cells. Homologous recombination was successful in two independent embryonic stem cell lines (lines 133 and 190). Positive chimeric male mice were then crossed with female C57BL/6J (B6) mice to produce *wfs1* heterozygous mice. Initial analyses demonstrated essentially the same phenotypes between the two lines, and therefore we have analyzed line 133 mice. In order to analyze animals with as homogenous a genetic background as possible, male *wfs1* heterozygous mice were backcrossed with female B6 mice for five successive generations. We also analyzed *wfs1* homozygous mice on the [(129Sv × B6) × B6]F2 hybrid background. The mice were kept in standard, specific pathogen-free conditions under a constant dark/light cycle. All animal experiments were approved by the local ethical committee for animal research at the Tohoku University.

Physiological studies

Control animals were age-matched siblings. Blood glucose levels in the non-fasting state were measured at 9:00–10:00 a.m. using a GluTest blood glucose monitor (Sanwa Chemicals, Tokyo, Japan). Serum insulin levels were determined by radioimmunoassay using a rat insulin RIA kit (Linco Research, St Charles, MO, USA). For oral glucose tolerance tests, animals after a 6 h fast were administered with 20% glucose solution (2 mg/g body weight) by gastric tubes. Whole-blood samples were collected from the tail tip at the indicated time points. Insulin tolerance tests were performed after a 6 h fast by an intraperitonial injection of human regular insulin (0.75 units/kg body weight).

Immunohistochemistry and morphometry

For brain sections, animals were anesthetized by ethylethel, and 4% formalin was perfused from the left ventricle. For pancreatic sections, the animals were killed by cervical dislocation. Dissected pancreas pieces were fixed in 4% formalin. Formalin-fixed paraffin-embedded sections of pancreas were de-paraffinized and re-hydrated. For insulin and glucagon staining, the sections were then incubated with a guinea pig anti-insulin IgG (DAKO Japan, Kyoto, Japan) diluted 1 : 1000 and a mouse anti-glucagon IgG (Sigma-Aldrich Japan, Tokyo, Japan) diluted 1 : 2000 for 1 h at room temperature. The anti-insulin and -glucagon primary antibodies were followed by a 45 min incubation with a fluorescein isothiocyanate (FITC)-conjugated anti-guinea pig IgG and a Texas Red-conjugated anti-mouse IgG (Jackson ImmunoResearch, West Grove, PA, USA). The antibody raised against the 290 amino acid α-mWFS1-N was described previously (30). Pancreatic sections incubated with the anti-WFS1 antibody were then stained with an FITC-conjugated anti-rabbit IgG (Jackson ImmunoResearch). Immunohistochemical analyses were performed, sacrificing at least four different animals for each condition. For measurements of β-cell area, more than 10 pancreatic tissue sections per animal were randomly selected, stained with anti-insulin IgG and eosin. Pancreatic area and β-cell area were each estimated using the intensity thresholding function of the NIH Image software. Four animals were analyzed for each group.

Pancreatic insulin and glucagon content

Pancreases were suspended in cold acid ethanol and minced by scissors, and left at −20°C for 48 h, with sonication every 24 h. Insulin content in the acid ethanol supernatant was determined with a rat insulin RIA Kit (Linco Research). Glucagon content in the same extract was measured by a glucagon RIA kit (Linco Research).

Islet studies

Construction of a recombinant adenovirus expressing murine WFS1 protein. A recombinant adenovirus AdCAGmWFS1, bearing an *EcoR*I fragment of murine WFS1 cDNA, was constructed by the method described previously (31,32). AdCAGlacZ expressing β-galactosidase was used as a control adenovirus. Isolated islets were infected with the recombinant adenoviruses at 1.2×10^5 particles per islet in 1.0 ml medium for 60 min.

Isolation and static incubation of islets. Islets isolated from age-matched wild-type and mutant siblings at 14–17 weeks were isolated by retrograde injection of collagenase (Serva, Heidelberg, Germany) into the pancreatic duct according to standard procedures. For secretion studies, batches of 10 islets (triplicates for each condition) were kept in Krebs–Ringer-bicarbonate-HEPES buffer [KRBH; 140 mM NaCl, 3.6 mM KCl, 0.5 mM NaH_2PO_4, 0.5 mM $MgSO_4$, 1.5 mM $CaCl_2$, 2 mM $NaHCO_3$, 10 mM HEPES (pH 7.4)] containing 0.1% BSA and stimulators indicated. Islet insulin content was measured following extraction by acid ethanol. Insulin was detected by radioimmunoassay.

Single cell Ca^{2+} measurement. Islets isolated from mice at 12–16 weeks were dispersed, plated on glass-bottomed dishes and cultured for 3 days before measurement. β-Cells were identified by adenovirus-mediated expression of green fluorescent protein driven by the insulin promoter (33). We performed experiments without adenovirus-mediated expression of green fluorescent protein, identifying β-cells with immunostaining after perfusion, and observed similar results (data not shown). Cells were incubated with 1 μM Fura 2-AM (Dojindo, Kumamoto, Japan) for 30 min, perfused with KRBH and excited at 340 and 380 nm. A cooled CCD camera (Hamamatsu Photonics, Shizuoka, Japan) mounted on a microscope (Leica Microsystems, Heerbrugg, Switzerland) was used to capture fluorescence images. Ca^{2+} rises were compared by calculating areas between Ca^{2+} curves and baselines for the 300 s after the onset of Ca^{2+} rises.

LM-PCR amplification of DNA fragments. Groups of 50 islets isolated from mice at 15–17 weeks of age were cultured for 3 days in RPMI with different glucose concentrations. In another series of experiments, groups of 50 islets were treated with 2 μg/ml tunicamycin (Sigma-Aldrich Japan), 2 μM thapsigargin (Alamone Labs, Jerusalem, Israel) or a combination of interferon-γ (100 units/ml; PeproTech, London, UK) and tumor necrosis factor-α (500 units/ml; PeproTech). Genomic DNA was isolated from treated islets using the DNeasy kit (Qiagen-Japan, Tokyo, Japan). The PicoGreen® dsDNA quantitation kit (Molecular Probes, Eugene, OR, USA) was used to determine the DNA concentrations. 200 ng of the genomic DNA was ligated with an adaptor, which has been generated by annealing two synthetic oligonucleotides 5′-AGCACTCTCGAGCCTCT CACCGCA-3′ and 5′-TGCGGTGAGAGG-3′. A portion of ligation mixture (30%) was used for the PCR amplification with a primer 5′-AGCACTCTCGAGCCTCTCACCGCA-3′. The resulting PCR products were run on 1.2% agarose gels. Intensities of ladders between 500 and 1000 bp were analyzed using the Scion Image software. In order to compare data from separate gels, band intensity was normalized to the average laddering of the control islets at 5 mM glucose.

Statistical analyses

Data are presented as mean ± SE, unless otherwise noted. Differences between wild-type and mutant animals were assessed by Student's *t*-test.

ACKNOWLEDGEMENTS

We thank Professor H. Takeshima, Dr Y. Ohwada and Professor T. Itoh, Tohoku University, for their help in Ca^{2+} imaging and immunohistochemical analyses. We are also grateful to N. Nishino, T. Wadatsu and N. Miyazawa, Otsuka GEN Research Institute, for their help in generation of WFS1-deficient mice. Y. Takahashi is gratefully acknowledged for her excellent technical assistance. This study was supported by Grants in Aid for Scientific Research (13204062) to Y.O. from the Ministry of Education, Science, Sports and Culture of Japan.

REFERENCES

1. Wolfram, D.J. and Wagener, H.P. (1938) Diabetes mellitus and simple optic atrophy among siblings: report on four cases. *Mayo Clinic Proc.*, **13**, 715–718.
2. Swift, M. and Swift, R.G. (2001) Psychiatric disorders and mutations at the Wolfram syndrome locus. *Biol. Psychiatry*, **47**, 787–793.
3. Inoue, H., Tanizawa, Y., Wasson, J., Behn, P., Kalidas, K., Bernal-Mizrachi, E., Mueckler, M., Marshall, H., Donis-Keller, H., Crock, P. *et al.* (1998) A gene encoding a transmembrane protein is mutated in patients with diabetes mellitus and optic atrophy (Wolfram syndrome). *Nat. Genet.*, **20**, 143–148.
4. Strom, T.M., Hoetnagael, K., Hofmann, S., Gekeler, F., Scharfe, C., Rabl, W., Gerbitz, K.D. and Meitinger, T. (1998) Diabetes insipidus, diabetes mellitus, optic atrophy and deafness (DIDMOAD) caused by mutations in a novel gene (wilframin) coding for a predicted transmembrane protein. *Hum. Mol. Genet.*, **7**, 2021–2028.
5. Cryns, K., Sivakumaran, T.A., Van den Ouweland, J.M., Pennings, R.J., Cremers, C.W., Flothmann, K., Young, T.L., Smith, R.J., Lesperance, M.M. and Van Camp, G. (2003) Mutational spectrum of the *WFS1* gene in Wolfram syndrome, nonsyndromic hearing impairment, diabetes mellitus, and psychiatric disease. *Hum. Mut.*, **22**, 275–287.
6. Bespalova, I.N., Van Camp, G., Bom, S.J., Brown, D.J., Cryns, K., DeWan, A.T., Erson, A.E., Flothmann, K., Kunst, H.P., Kurnool, P. *et al.* (2001) Mutations in the Wolfram syndrome 1 gene (WFS1) are a common cause of low frequency sensorineural hearing loss. *Hum. Mol. Genet.*, **15**, 2501–2508.
7. Young, T.L., Ives, E., Lynch, E., Person, R., Snook, S., MacLaren, L., Cater, T., Griffin, A., Fernandez, B., Lee, M.K. *et al.* (2001) Non-syndromic progressive hearing loss DFNA38 is caused by heterozygous missense mutation in the Wolfram syndrome gene *WFS1*. *Hum. Mol. Genet.*, **15**, 2509–2514.
8. Ohta, T., Koizumi, A., Kayo, T., Shoji, Y., Watanabe, A, Monoh, K., Higashi, K., Ito, S., Ogawa, O., Wada, Y. *et al.* (1998) Evidence of an increased risk of hearing loss in heterozygous carriers in a Wolfram syndrome family. *Hum. Genet.*, **103**, 470–474.
9. Minton, J.A., Hattersley, A.T., Owen, K., McCarthy, M.I., Walker, M., Latif, F., Barrett, T. and Frayling, T.M. (2002) Association studies of genetic variation in the *WFS1* gene and type 2 diabetes in U.K. populations. *Diabetes*, **51**, 1287–1290.
10. Awata, T., Inoue, K., Kurihara, S., Ohkubo, T., Inoue, I., Abe, T., Takino, H., Kanazawa, Y. and Katayama, S. (2000) Missense variations of the gene responsible for Wolfram syndrome (WFS1/wolframin) in Japanese: possible contribution of the Arg456His mutation to type 1 diabetes as a nonautoimmune genetic basis. *Biochem. Biophys. Res. Commun.*, **268**, 612–616.
11. Sequeira, A. Kim, C., Seguin, M., Lesage, A., Chawky, N., Desautels, A., Tousignant, M., Vanier, C., Lipp, O., Benkelfat, C. *et al.* (2003) Wolfram syndrome and suicide: evidence for a role of WFS1 in suicidal and impulsive behavior. *Am. J. Mol. Genet.*, **119B**, 108–113.
12. Takeda, K., Inoue, H., Tanizawa, Y., Matsuzaki, Y., Oba, J., Watanabe, Y., Shinoda, K. and Oka, Y. (2001) WFS1 (Wolfram syndrome 1) gene product: predominant subcellular localization to endoplasmic reticulum in cultured cells and neuronal expression in rat brain. *Hum. Mol. Genet.*, **10**, 477–484.
13. Hofmann, S., Philbrook, C., Gerbitz, K.D. and Bauer, M.F. (2003) Wolfram syndrome: structural and functional analyses of mutant and wild-type wolframin, the WFS1 gene product. *Hum. Mol. Genet.*, **12**, 2003–2012.

14. Kaufmann, R. (2002) Orchestrating the unfolded protein response in health and disease. *J. Clin. Invest.*, **110**, 1389–1398.
15. Harding, H.P. and Ron, D. (2002) Endoplasmic reticulum stress and the development of diabetes. *Diabetes*, **51** (Suppl. 3), S455–S461.
16. Rando, T.A., Horton, J.C. and Layzer, R.B. (1992) Wolfram syndrome: evidence of a diffuse neurodegenerative disease by magnetic resonance imaging. *Neurology*, **42**, 1220–1224.
17. Karasik, A., O'Hara, C., Srikanta, S., Swift, M., Soeldner, J.S., Kahn, C.R. and Herskowitz, R.D. (1989) Genetically programmed selective islet beta-cell loss in diabetic subjects with Wolfram's syndrome. *Diabetes Care*, **12**, 135–138.
18. Ferri, K.F. and Koemer, G. (2001) Organelle-specific initiation of cell death pathways. *Nat. Cell Biol.*, **3**, E255–E263.
19. Coleman, D.L. (1982) Diabetes–obesity syndromes in mice. *Diabetes*, **31** (Suppl. 2), 1–6.
20. Terauchi, Y., Matsui, J., Suzuki, R., Kubota, N., Komeda, K., Aizawa, S., Eto, K., Kimura, S., Nagai, R., Tobe, K. *et al.* (2003) Impact of genetic background and ablation of insulin receptor substrate (IRS)-3 on IRS-2 knock-out mice. *J. Biol. Chem.*, **278**, 14284–14290.
21. Ishihara, H., Tashiro, F., Ikuta, K., Asano, T., Katagiri, H., Inukai, K., Kikuchi, M., Yazaki, Y., Oka, Y. and Miyazaki, J. (1995) Inhibition of pancreatic beta-cell glucokinase by antisense RNA expression in transgenic mice: mouse strain-dependent alteration of glucose tolerance. *FEBS Lett.*, **371**, 329–332.
22. Kulkarni, R.N., Almind, K., Goren, H.J., Winnay, J.N., Ueki, K., Okada, T. and Kahn, C.R. (2003) Impact of genetic background on development of hyperinsulinemia and diabetes in insulin receptor/insulin receptor substrate-1 double heterozygous mice. *Diabetes*, **52**, 1528–1534.
23. Wier, G.C., Bonner-Wier, S. and Leahy, J.L. (1990) Islet mass and function in diabetes and transplantation. *Diabetes*, **39**, 401–405.
24. Osman, A.A., Saito, M., Makepeace, C, Permutt, M.A., Schlesinger, P. and Mueckler, M. (2003) Wolframin expression induces novel ion channel activity in endoplasmic reticulum membranes and increases intracellular calcium. *J. Biol. Chem.*, **278**, 52755–52762.
25. Reddy, S. Bradley, J., Ginn, S., Pathipati, P. and Ross, J.M. (2003) Immunohistochemical study of caspase-3-expressing cells within the pancreas of non-obese diabetic mice during cyclophosphamide-accelerated diabetes. *Histochem. Cell Biol.*, **119**, 451–461.
26. Donath, M.Y., Gross, D.J., Cerasi, E. and Kaiser, N. (1999) Hyperglycemia-induced beta-cell apoptosis in pancreatic islets of *Psammomys obesus* during development of diabetes. *Diabetes*, **48**, 738–744.
27. Maedler, K., Sergeev, P., Ris, F., Oberholzer, J., Joller-Jemelka, H.I., Spinas, G.A., Kaiser, N., Halban, P.A. and Donath, M.Y. (2002) Glucose-induced beta cell production of IL-1beta contributes to glucotoxicity in human pancreatic islets. *J. Clin. Invest.*, **110**, 851–860.
28. Harding, H.P., Zeng, H., Xhang, Y., Jungries, R., Chung, P., Plesken, H., Sabatini, D.D. and Ron, D. (2001) Diabetes mellitus and exocrine pancreatic dysfunction in *Perk*$^{-/-}$ mice reveals a role for translational control in secretory cell survival. *Mol. Cell*, **7**, 1153–1163.
29. Butler, A.E., Janson, J., Bonner-Weir, S., Ritzel, R., Rizza, R.A. and Butler, P.C. (2003) β-Cell deficit and increased β-cell apoptosis in humans with type 2 diabetes. *Diabetes*, **52**, 102–110.
30. Cryns, K., Thys, S., van Laer, L., Oka, Y., Pfister, M., van Nassauw, L., Smith, R.J.H., Timmermans, J.P. and Van Camp, G. (2003) The *WFS1* gene, responsible for low frequent sensorineural hearing loss and Wolfram syndrome, is expressed in a variety of inner ear cells. *Histochem. Cell Biol.*, **119**, 247–256.
31. Miyake, S., Makimura, M., Kanegae, Y., Harada, S., Sato, Y., Takamori, K., Tokuda, C. and Saito, I. (1996) Efficient generation of recombinant adenoviruses using adenovirus DNA–terminal protein complex and a cosmid bearing the full-length virus genome. *Proc. Natl Acad. Sci. USA*, **93**, 1320–1324.
32. Niwa, H., Yamamura, K. and Miyazaki, J. (1991) Efficient selection for high-expression transfectants with a novel eukaryotic vector. *Gene*, **108**, 193–199.
33. Ishihara, H., Maechler, P., Gjinovci, A., Herrera, P.-L. and Wollheim, C.B. (2003) Islet β-cell secretion determines glucagon secretion from the neighboring α-cells. *Nat. Cell Biol.*, **5**, 330–335.

Available online at www.sciencedirect.com
SCIENCE DIRECT®
ELSEVIER
Biochemical and Biophysical Research Communications 325 (2004) 250–256
BBRC
www.elsevier.com/locate/ybbrc

Endoplasmic reticulum stress and N-glycosylation modulate expression of WFS1 protein

Suguru Yamaguchi[a], Hisamitsu Ishihara[a,*], Akira Tamura[a], Takahiro Yamada[a], Rui Takahashi[a], Daisuke Takei[a], Hideki Katagiri[b], Yoshitomo Oka[a]

[a] *Division of Molecular Metabolism and Diabetes, Tohoku University Graduate School of Medicine, 2-1 Seiryo-machi, Aoba-ku, Sendai, Miyagi 980-8575, Japan*

[b] *Division of Advanced Therapeutics for Metabolic Diseases, Tohoku University Graduate School of Medicine, 2-1 Seiryo-machi, Aoba-ku, Sendai, Miyagi 980-8575, Japan*

Received 22 September 2004
Available online 22 October 2004

Abstract

Mutations of the *WFS1* gene are responsible for two hereditary diseases, Wolfram syndrome and low frequency sensorineural hearing loss. The WFS1 protein is a glycoprotein located in the endoplasmic reticulum (ER) membrane but its function is poorly understood. Herein we show WFS1 mRNA and protein levels in pancreatic islets to be increased with ER-stress inducers, thapsigargin and dithiothreitol. Another ER-stress inducer, the N-glycosylation inhibitor tunicamycin, also raised WFS1 mRNA but not protein levels. Site-directed mutagenesis showed both Asn-663 and Asn-748 to be N-glycosylated in mouse WFS1 protein. The glycosylation-defective WFS1 protein, in which Asn-663 and Asn-748 had been substituted with aspartate, exhibited an increased protein turnover rate. Consistent with this, the WFS1 protein was more rapidly degraded in the presence of tunicamycin. These data indicate that ER-stress and N-glycosylation play important roles in WFS1 expression and stability, and also suggest regulatory roles for this protein in ER-stress induced cell death.

Keywords: Wolfram syndrome; Low frequency sensorineural hearing loss; WFSI; ER-stress; N-Glycosylation

The *WFS1* gene, encoding a transmembrane protein of the endoplasmic reticulum (ER) [1], is mutated in two hereditary diseases, autosomal recessive Wolfram syndrome (OMIN:222300) [2,3] and autosomal dominant low frequency sensorineural hearing loss (LFSNHL) (OMIM:600965) [4,5]. The former is also known as DIDMOAD, summarizing the most frequent symptoms; diabetes insipidus, diabetes mellitus, optic atrophy, and deafness. More than 100 mutations of the *WFS1* gene have been identified to date in patients with these diseases [6]. WFS1 protein, also called wolframin, consists of 890 amino acids [2,3] and its homologues are found in several organisms; *Drosophila melanogaster* (CG4917), *Anopheles gambiae* (EBIP3764), *Ciona intestinalis* (Cin.16116), *Fugu rubripes* (SINFRUP82345), and *Xenopus laevis* (Xl.3995). However, these proteins share no homology with known proteins, making it difficult to speculate as to their functions.

We recently established a murine model with a disrupted *wfs1* gene [7]. Mutant mice exhibited impaired glucose homeostasis due to defective insulin secretion in vivo. Studies using isolated islets revealed that mutant islet cells were prone to apoptosis induced by insults which impair ER functions and trigger the so-called unfolded protein response (UPR) [8,9]. Therefore, it was suggested that WFS1 protein plays a role in modulation of apoptotic processes that arise from impairment of ER function [7]. In addition, isolated islets from WFS1-deficient mice exhibited defective insulin

* Corresponding author. Fax: +81 22 717 7612.
E-mail address: ishihara-tky@umin.ac.jp (H. Ishihara).

0006-291X/$ - see front matter © 2004 Elsevier Inc. All rights reserved.
doi:10.1016/j.bbrc.2004.10.017

secretion which was accompanied by decreased calcium responses to glucose. Conversely, wolframin-overexpressing islets showed increased insulin secretion, indicating that wolframin also participates in regulation of stimulus-secretion coupling in insulin exocytosis [7]. It has recently been reported that WFS1 protein/wolframin expression in *Xenopus* oocytes conferred cation channel activity and increased cytosolic calcium levels [10]. This observation is intriguing since intracellular calcium regulation plays important roles in modulating both apoptotic and exocytotic processes. Despite these advancements, however, little is known about the mechanisms by which WFS1 protein actually alters these processes.

To understand the role that WFS1 protein/wolframin plays in the regulation of apoptotic and exocytotic events as well as in other as yet unknown cellular processes, information on the structure and function of this protein must be obtained. The amino acid sequence suggests that WFS1 protein is a multi-membrane spanning protein with hydrophilic amino (N)- and carboxy (C)-terminal regions [2,3]. In addition, biochemical and immunocytochemical analyses showed WFS1 protein to be an ER membrane glycoprotein [1].

In the present studies, we first examined WFS1 protein expression after treatment with agents that trigger UPR. We found WFS1 mRNA and protein levels to be increased by thapsigargin or dithiothreitol (DTT). Treatment with tunicamycin, an inhibitor of N-glycosylation, also raised WFS1 mRNA levels, suggesting that UPR increases WFS1 mRNA levels. However, the WFS1 protein level is not increased by tunicamycin. Subsequent analyses demonstrated protein stability to be reduced in the glycosylation-defective WFS1 protein. These results contribute to further understanding of the functions of this enigmatic protein.

Materials and methods

Reagents and antibodies. Tunicamycin, thapsigargin, DTT, and anti-actin antibody were purchased from Sigma–Aldrich Japan (Tokyo, Japan). Anti-HA and anti-CHOP antibodies were obtained from Santa Cruz Biotechnology (Santa Cruz, CA). Anti-WFS1 N-terminus antibody was described previously [11].

Pancreatic islet isolation and treatment with ER-stress inducers. Pancreatic islets were isolated from male C57BL/6 mice by retrograde injection of collagenase (Sigma–Aldrich Japan, Tokyo, Japan) into the pancreatic duct. Approximately 100 (for Western blot analyses) or 200 (for RNA extraction) islets were treated with 2 μg/ml thapsigargin, 5 mM DTT, or 5 μM tunicamycin for 36 h in RPMI1640 medium. Total RNA was extracted using Isogen reagent (NipponGene, Toyama, Japan). Quantitative real-time PCR analysis for WFS1 mRNA levels was performed using primers, 5′-CTGGAAACTCAACCCCAAGA-3′ and 5′-TTGGATTCACTGCTGACGAG-3′.

Plasmids. pHA-mWFS1 encodes a fusion protein consisting of an initiator methionine, the HA epitope tag (YPYDVPDYA), and amino acids 2–890 of mouse WFS1 protein. To generate this plasmid, a fragment encoding a *Sal*I restriction site and amino acids 2–484 was amplified by PCR. Using the PCR method, pmWFS1-HA encoding mouse WFS1 protein with an HA tag between residues 830 and 831 was also generated. pHA-mWFS1(N633D) and pHA-mWFS1 (N748D), which encode HA-tagged WFS1 protein with a mutation of asparagine 633 to aspartate and asparagine 748 to aspartate, respectively, were generated using PCR-based mutagenesis on pHA-mWFS1. pHA-mWFS1(N633D/N748D) encoding a mutant protein with mutation of both asparagine residues was generated using pHA-mWFS1(N633D).

Cell culture and transient transfection. MIN6 [12] and COS7 cells were grown in Dulbecco's modified Eagle's medium (DMEM) supplemented with 10% (v/v) fetal calf serum, 50 U/ml penicillin, and 50 μg/ml streptomycin sulfate. Transfection of plasmids was carried out using FuGENE6 (Roche, Indianapolis, IN) diluted in OPTI media (Invitrogen, Carlsbad, CA). Cells were harvested for Western blot or proceeded to immunostaining analysis 36 h after transfection. Immunostaining was performed using anti-HA antibody and FITC-conjugated anti-mouse IgG (Jackson ImmunoResearch, West Grove, PA).

Trypsin treatment. COS7 cells transfected with either pHA-mWFS1 or pmWFS1-HA were homogenized in a buffer containing 270 mM sucrose, 2 mM EDTA, and 50 mM Hepes (pH 7.5). Cellular membranes were recovered by centrifuging the homogenate at 17,400*g* for 15 min. Membranes (100 μg) were then incubated with trypsin at various concentrations at 4 °C. After a 30 min incubation, homogenates were boiled and subjected to SDS/PAGE and Western blot analysis.

Endoglycosydase cleavage. COS7 cells transfected with either wild-type WFS1 cDNA or mutant constructs were dissolved in denaturing buffer (0.5% SDS, 1% β-mercaptoethanol), boiled for 10 min at 100 °C, then incubated at 37 °C for 1 h with endoglycosidase H (500 U), and subjected to electrophoresis on NuPAGE 3–8% Tris–acetate gel (Invitrogen).

Metabolic labeling. MIN6 cells were labeled with [^{35}S]methionine and [^{35}S]cysteine (100 μCi/ml; EXPRE^{35}S^{35}S labeling mix, Perkin–Elmer-New England Nuclear, Boston, MA) in DMEM with either methionine or cysteine in the presence or absence of 5 μg/ml tunicamycin for 3 h. Cells were then chased for different periods in complete medium with or without tunicamycin. COS7 cells transfected with pHA-mWFS1 or pHA-mWFS1(N633D/N748D) were also labeled with [^{35}S]methionine and [^{35}S]cysteine for 3 h. Cells were then chased for different periods in complete medium. MIN6 and COS7 cells were lysed in a buffer containing 100 mM NaCl, 0.5 mM EDTA, 20 mM Tris (pH 7.5), and 0.5% NP-40. Lysates were incubated with 10 μl protein A/G–Sepharose (Amersham Biosciences, Piscataway, NJ) for 2 h and then briefly centrifuged. The resulting supernatant was incubated with anti-WFS1 N-terminus or anti-HA antibodies overnight and then incubated with protein A/G–Sepharose for 2 h. The beads were washed three times and bound WFS1 proteins were eluted in SDS-sample buffer and subjected to SDS/PAGE (10%).

Statistical analyses. Data are presented as means ± SE. Differences were assessed by Student's *t* test.

Results and discussion

Effect of ER-stress inducers on WFS1 expression in pancreatic islets

We recently reported that WFS1-deficient islets exhibited increased susceptibility to apoptosis due to impaired ER function [7]. Therefore, in this study, we first determined WFS1 expression in isolated mouse pancreatic islets treated with the ER-stress inducers, thapsigargin, DTT, and tunicamycin. Thapsigargin is an inhibitor of the sarco(endo)plasmic reticulum Ca^{2+} pump and

depletes ER Ca^{2+}, which affects the functions of Ca^{2+}-dependent ER chaperone proteins. DTT and tunicamycin affect protein folding by disrupting disulfide bonds and inhibiting N-glycosylation, respectively. These compounds therefore cause mis-folding of proteins (ER-stress) and induce UPR [13]. As shown in Fig. 1, WFS1 protein expression was increased in islets treated with 2 μM thapsigargin (Fig. 1A) or 5 mM DTT (Fig. 1B) for 36 h. Greater than threefold increases in WFS1 mRNA levels were also observed by quantitative RT-PCR analyses in islets treated with these agents (data not shown). Another ER-stress inducer, tunicamycin (5 μg/ml), did not raise WFS1 protein levels in isolated islets (Fig. 1C). However, quantitative RT-PCR analyses revealed WFS1 mRNA levels to be increased by 72% in islets treated with tunicamycin (Fig. 1D). These data suggest that WFS1 mRNA expression increases in response to the ER-stress.

WFS1 protein has been shown to be a glycoprotein [1] like the inositol trisphosphate receptor, another ER membrane resident protein essential for cellular calcium homeostasis and signaling [14]. The unaltered WFS1 protein levels despite increased mRNA levels in islets treated with tunicamycin raise the possibility that inhibition of N-glycosylation affects WFS1 protein stability. To address this possibility, pancreatic β-cell derived MIN6 cells were labeled for 3 h with [^{35}S]methionine/cysteine and chased with unlabeled methionine and cysteine for different intervals in the continuous absence or presence of tunicamycin. As shown in Fig. 1E, WFS1 protein in tunicamycin-treated cells was more rapidly degraded, suggesting that inhibition of N-glycosylation reduces WFS1 protein stability.

Membrane topology of WFS1 protein

To study the roles of N-glycosylation more specifically, we first sought to determine N-glycosylation site(s) of WFS1 protein/wolframin. Since N-glycosylation occurs in the ER, it was prerequisite to know the membrane topology of this protein. The initial hydropathy plot studies did not provide a definitive answer; WFS1 protein contains 9 or 10 transmembrane segments, with long hydrophilic stretches on both the N- and the C-termini [2,3].

To localize the N- and the C-termini of WFS1 protein with respect to the ER membrane, we transiently expressed, in COS7 cells, mouse WFS1 protein tagged with an HA-epitope in either the N- or the C-terminal stretch (designated HA-mWFS1 or mWFS1-HA, respectively,

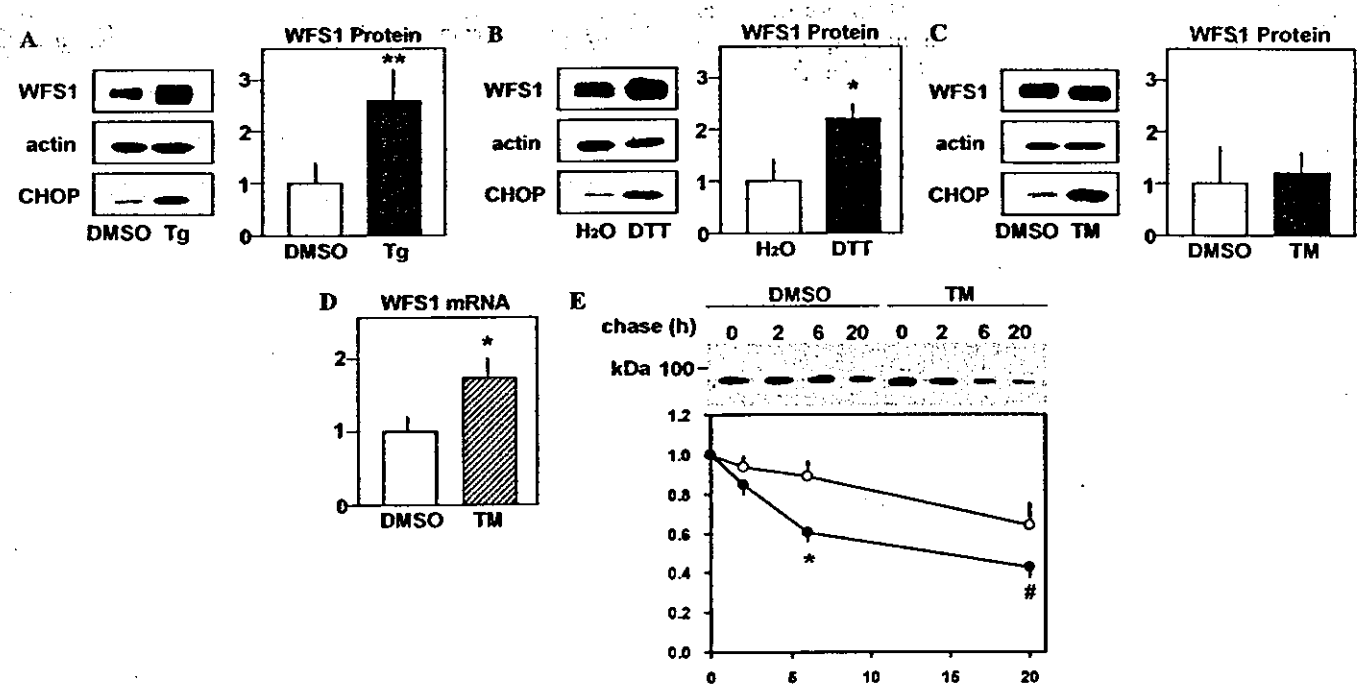

Fig. 1. WFS1 expression in mouse pancreatic islets in response to ER-stress inducers. (A–C) Isolated mouse islets were challenged with 2 μM thapsigargin (Tg) (A, $n = 4$), 5 mM DTT (B, $n = 3$) or 5 μg/ml tunicamycin (TM) (C, $n = 5$). After a 36-h incubation, the islets were subjected to SDS/PAGE and blotted using antibodies against the WFS1 N-terminus, actin, or CHOP. Representative blots are shown in the left panels. Increased CHOP expression indicated successful induction of ER-stress mediated apoptosis. WFS1 protein/actin levels are summarized in the right panels. Data are expressed as the expression relative to those of a control islet preparation. (D) Total RNA was extracted from isolated mouse islets treated with 5 μg/ml tunicamycin for 36 h. WFS1 and GAPDH mRNA levels were determined by quantitative real-time PCR. WFS1 mRNA levels were normalized to those of GAPDH. Data were obtained using three independent sets of islet preparations. (E) MIN6 cells were pulse-labeled for 3 h without or with 5 μg/ml tunicamycin and chased for up to 20 h in the continuous absence or presence of the drug. A representative result from three independent experiments is shown in the upper panel. Data from three experiments are summarized, after normalization to time zero of the chase in the lower panel. Open circles, DMSO-treated MIN6 cells. Closed circles, tunicamycin-treated cells. $^{\#}P = 0.0634$, $^{*}P < 0.05$, $^{**}P < 0.01$.

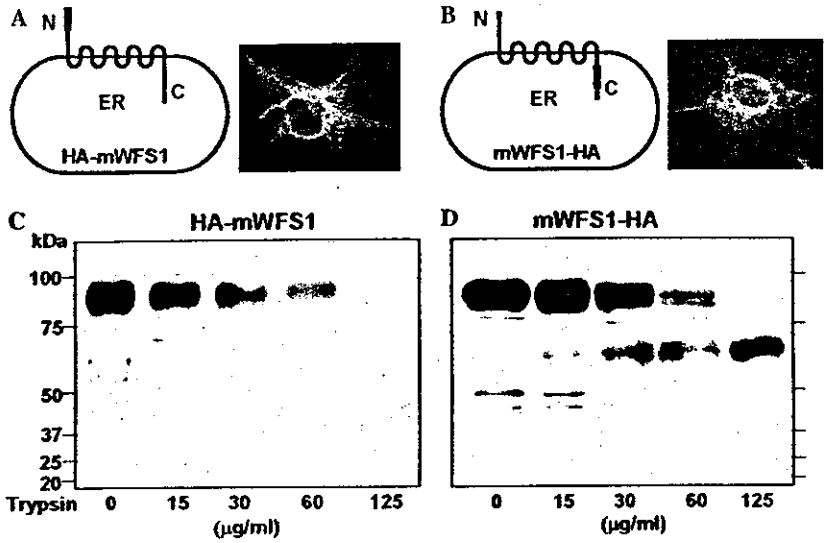

Fig. 2. Membrane orientations of the N- and the C-termini of WFS1 protein as determined by trypsin proteolysis. WFS1 protein tagged with the HA epitope at either the N- (A,C) or the C-terminus (B,D) was expressed in COS7 cells. (A,B) Schematic illustration and immunocytochemical demonstration of the HA-tagged WFS1 proteins used in (C) and (D). (C,D) Membranes from COS7 cells transfected with a plasmid encoding either HA-mWFS1 or mWFS1-HA were treated with the indicated amounts of trypsin. After incubation for 30 min at 4 °C, the reactions were stopped by boiling for 5 min, and subjected to SDS/PAGE and immunoblot analysis with anti-HA antibody.

Figs. 2A and B). HA-mWFS1 and mWFS1-HA proteins were successfully expressed and localized to the ER, as demonstrated by reticular staining in the cytoplasm (Figs. 2A and B). Membrane preparation of cells expressed with either HA-mWFS1 or mWFS1-HA proteins was then subjected to trypsin digestion followed by SDS/PAGE and immunoblotting with an antibody against the HA epitope. The HA-epitope tagged at the N-terminus was completely digested with increasing concentrations of trypsin (Fig. 2C). This was not due to loss of membrane vesicle integrity, since no changes in an ER-resident chaperone protein, GRP78, were detected using an antibody against GRP78 in the same membrane preparations (data not shown). In contrast, the C-terminal HA epitope was protected from trypsin (Fig. 2D). These results indicated that WFS1 protein has odd numbers of transmembrane segments with the orientation of the N-terminus toward the cytoplasm and that of the C-terminus toward the ER lumen. A similar conclusion was obtained by trypsin-digestion of the membrane, followed by detection with C-terminal or N-terminal antibodies [15].

Determination of N-glycosylation sites.

Mouse WFS1 protein has six asparagine residues with the consensus sequence for N-glycosylation (N-X-S/T, where X is any amino acid except for proline). According to a 9-transmembrane model with N-terminus cytosolic/C-terminus luminal orientation, asparagines 663 and 748 would be localized in the ER. Therefore, we mutated these two asparagine residues to aspartate in order to determine whether one or both are N-linked glycosylation site(s). Mutant WFS1 proteins in which asparagine 663 and/or asparagine 748 was mutated to aspartate [designated HA-mWFS1(N663D), HA-mWFS1(N748D), and HA-mWFS1(N663D/N748D)] were successfully expressed in the ER (Fig. 3A). When these WFS1 mutant proteins were subjected to SDS/PAGE, HA-mWFS1(N663D/N748D) migrated faster than the HA-wild-type mWFS1 protein, while both HA-mWFS1(N663D) and HA-mWFS1(N748D) mutants were between the two (Fig. 3B). These results suggested that both asparagine residues, 663 and 748, are glycosylation sites and place the C-terminal stretch of WFS1 protein within the intraluminal compartment. Furthermore, as shown in Fig. 3C, although endoglycosidase H (Endo H) treatment of the wild-type WFS1 protein resulted in faster migration of the protein, the mobility of the double mutant [WFS1 (N663D/N748D)] protein was not affected by treatment with Endo H. In addition, the double mutant protein exhibited the same mobility as the wild-type WFS1 protein treated with Endo H. These data demonstrated that no asparagine residue other than N663 and N748 is glycosylated.

Reduced protein stability of N-glycosylation-defective WFS1 protein

N-glycosylation reportedly plays an important role in the stability of proteins such as the T cell antigen receptor α-subunit [16], the α-subunit of the nicotinic acetylcholine receptor [17], and apolipoprotein B [18]. Therefore, to assess the role of N-glycosylation in WFS1 protein stability, we performed pulse-chase

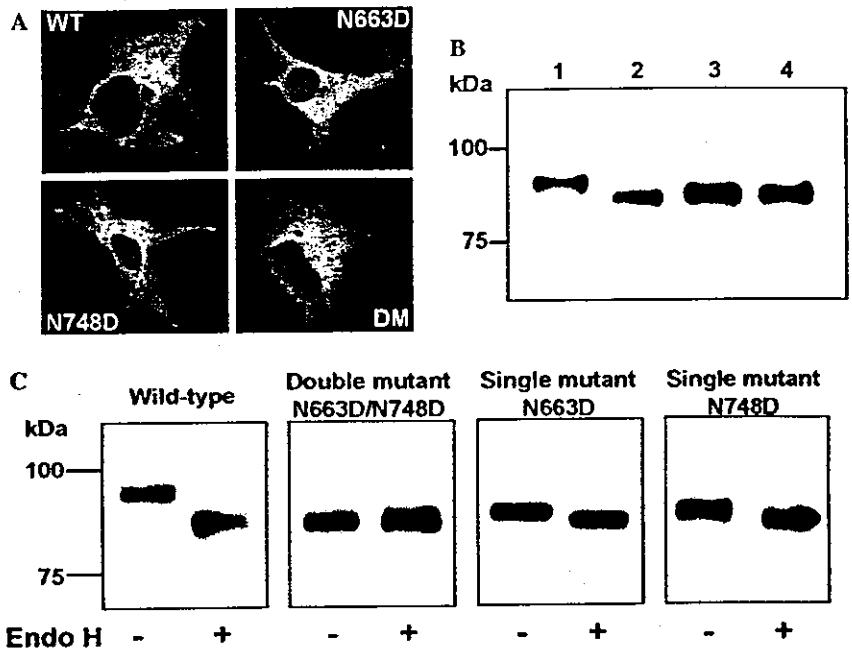

Fig. 3. Electrophoretic mobility and effect of endoglycosidase digestion on HA-tagged wild-type and mutant WFS1 proteins. (A) Immunofluorescence localization of HA-tagged WFS1 proteins: upper left, wild-type HA-mWFS1; upper right, HA-mWFS1(N663D); lower left, HA-mWFS1(N748D); lower right, HA-mWFS1(N663D/N748D). (B) COS7 cells transfected with 0.5 μg plasmids encoding either HA-tagged wild-type or mutant WFS1 proteins were lysed, subjected to SDS/PAGE, and probed with anti-HA antibody: lane 1, HA-mWFS1; lane 2, HA-mWFS1 (N663D/N748D); lane 3, HA-mWFS1(N663D); and lane 4, HA-mWFS1(N748D). (C) Lysates of COS7 cells transfected with either wild-type WFS1 cDNA or mutant constructs were incubated at 37 °C for 1 h with or without endoglycosidase H (500 U) and were subjected to electrophoresis on NuPAGE 3–8% Tris–acetate gel.

experiments. In these experiments, COS7 cells transiently transfected with either the HA-wild-type mWFS1 or mutant HA-mWFS1(N663D/N748D) cDNAs were labeled for 3 h with [^{35}S]methionine/cysteine and chased for different intervals. As shown in Fig. 4, the wild-type mWFS1 protein was relatively stable; 65 ± 6% ($n = 3$) of the protein remained 18 h after its synthesis. In contrast, only 44 ± 5% ($n = 3$) of mWFS1(N663D/N748D) remained after 18 h. These data showed protein stability to be reduced when both N-glycosylation sites were disrupted. One could argue an increased turnover rate of mWFS1(N663D/N748D) to be due to introducing aspartate residues rather than lack of glycosylation. To study the roles of N-glycosylation in various glycoproteins, asparagine residues in the consensus motif have been substituted with a variety of amino acids, such as aspartate ([19,20], this study), glutamine [14,21], alanine [19,22], threonine [23], and isoleucine [24]. None of these replacements were perfect, because introducing different residues might have its own effects. In this study, we also observed that WFS1 protein in MIN6 cells was more rapidly degraded when treated with a glycosylation inhibitor, tunicamycin (Fig. 1E). Thus, both molecular and biochemical approaches indicated that glycosylation-defective WFS1 protein has reduced stability. We therefore conclude that N-glycosylation affects WFS1 protein levels. A previous study using the ER resident glycoprotein ribophorin showed N-glycosylation to be necessary for calnexin binding, which prevents the glycoprotein from being rapidly degraded [25]. Such a mechanism could also be operative in WFS1 protein.

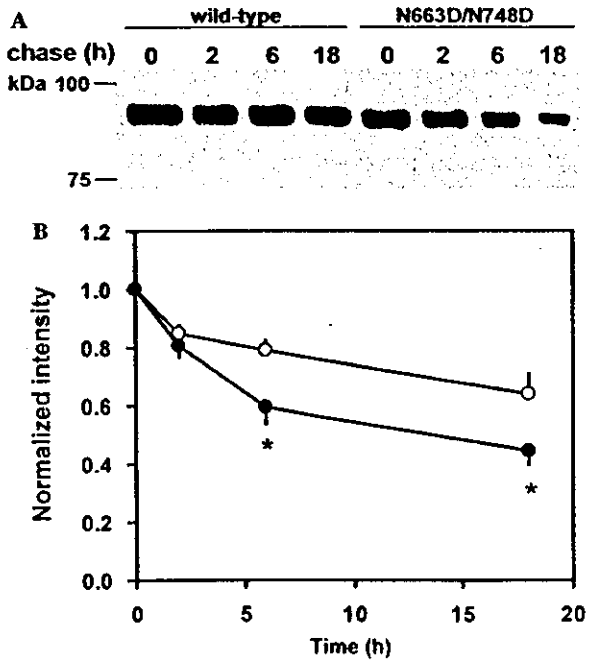

Fig. 4. Decreased stability of glycosylation-defective WFS1 protein. (A) HA-mWFS1 and HA-mWFS1(N663D/N748D) profiles of radiolabeled bands as a function of time of chase. A representative result from three experiments is shown. (B) Data from three experiments are summarized after normalization to time zero of chase. *$P < 0.05$.

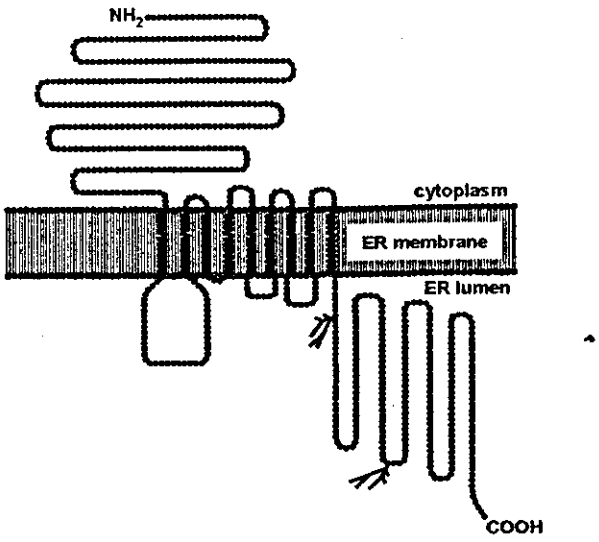

Fig. 5. Transmembrane topology model for mouse WFS1 protein with glycosylation sites. Membrane topology of mouse WFS1 protein as based on analysis using the SOSUI computer program [26] and data obtained in this study. Two N-glycosylation sites in the C-terminus stretch are depicted.

Herein, we defined the membrane topology of WFS1 by analyzing protease protection susceptibility: the orientation of the N-terminus in the cytoplasm and the C-terminus in the ER. This topology was supported by determining the N-glycosylation sites to be N663 and N748. A schematic diagram of WFS1 protein deduced from the current study and others is shown in Fig. 5. WFS1 protein/wolframin is a type II transmembrane protein and has long N-terminal and C-terminal stretches. These stretches could interact with other molecule(s), thereby mediating specific functions. Further study of these actions is clearly warranted. N663 and N748 residues in murine WFS1 protein correspond to N661 and N746 in the human orthologue. Although more than 100 mutations have been identified in WFS1 protein/wolframin and span the entire coding sequence, no mutations in these asparagine residues or adjacent amino acids were found in patients with Wolfram syndrome or LFSNHL. Given that loss of the functions of this protein is at least one of the pathogenic mechanisms of Wolfram syndrome [6,15], future survey of genomic sequences in patients with these diseases might identify mutations in these glycosylation sites.

The present data also provide evidence that increased WFS1 expression is the primary response of this protein to ER stress. There is no increase in WFS1 protein expression in response to tunicamycin, despite increased WFS1 mRNA levels. This is apparently attributable to the combined effects of increased mRNA levels and reduced protein stability. The increased WFS1 expression in response to ER-stress raises the possibility that WFS1 protein is a component of the UPR and plays a protective role against ER stress. This notion is supported by our recent findings that islets isolated from WFS1-deficient mice exhibited increased susceptibility to ER stress-induced apoptosis [7].

Acknowledgments

We are grateful to Y. Nagura for her expert technical assistance. This work was supported by a grant from Suzuken Memorial Foundation to H.I. and a Grant-in-Aid for Scientific Research (13204062) to Y.O. from the Ministry of Education, Science, Sports and Culture of Japan.

References

[1] K. Takeda, H. Inoue, Y. Tanizawa, Y. Matsuzaki, J. Oba, Y. Watanabe, K. Shinoda, Y. Oka, WFS1 (Wolfram syndrome 1) gene product: predominant subcellular localization to endoplasmic reticulum in cultured cells and neuronal expression in rat brain, Hum. Mol. Genet. 10 (2001) 477–484.

[2] H. Inoue, Y. Tanizawa, J. Wasson, P. Behn, K. Kalidas, E. Bernal-Mizrachi, M. Mueckler, H. Marshall, H. Donis-Keller, P. Crock, D. Rogers, M. Mikuni, H. Kimashiro, K. Higashi, G. Sobue, Y. Oka, M.A. Permutt, A gene encoding a transmembrane protein is mutated in patients with diabetes mellitus and optic atrophy (Wolfram syndrome), Nat. Genet. 20 (1998) 143–148.

[3] T.M. Strom, K. Hoetnagael, S. Hofmann, F. Gekeler, C. Scharfe, W. Rabl, K.D. Gerbitz, T. Meitinger, Diabetes insipidus, diabetes mellitus, optic atrophy and deafness (DIDMOAD) caused by mutations in a novel gene (wolframin) coding for a predicted transmembrane protein, Hum. Mol. Genet. 7 (1998) 2021–2028.

[4] I.N. Bespalova, G. Van Camp, S.J. Bom, D.J. Brown, K. Cryns, A.T. DeWan, A.E. Erson, K. Flothmann, H.P. Kunst, P. Kurnool, T.A. Sivakumaran, W.W.R.J. Cremers, S.M. Leal, M. Burmeister, M.M. Lesperance, Mutations in the Wolfram syndrome 1 gene (*WFS1*) are a common cause of low frequency sensorineural hearing loss, Hum. Mol. Genet. 15 (2001) 2501–2508.

[5] T.L. Young, E. Ives, E. Lynch, R. Person, S. Snook, L. MacLaren, T. Cater, A. Griffin, B. Fernandez, M.K. Lee, M.-C. King, Non-syndromic progressive hearing loss DFNA38 is caused by heterozygous missense mutation in the Wolfram syndrome gene WFS1, Hum. Mol. Genet. 15 (2001) 2509–2514.

[6] K. Cryns, T.A. Sivakumaran, J.M. Van den Ouweland, R.J. Pennings, C.W. Cremers, K. Flothmann, T.L. Young, R.J. Smith, M.M. Lesperance, G. Van Camp, Mutational spectrum of the WFS1 gene in Wolfram syndrome, nonsyndromic hearing impairment, diabetes mellitus, and psychiatric disease, Hum. Mutat. 22 (2003) 275–287.

[7] H. Ishihara, S. Takeda, A. Tamura, R. Takahashi, S. Yamaguchi, D. Takei, T. Yamada, H. Inoue, H. Soga, H. Katagiri, Y. Tanizawa, Y. Oka, Disruption of the WFS1 gene in mice causes progressive beta-cell loss and impaired stimulus-secretion coupling in insulin secretion, Hum. Mol. Genet. 13 (2004) 1159–1170.

[8] R. Kaufmann, Orchestrating the unfolded protein response in health and disease, J. Clin. Invest. 110 (2002) 1389–1398.

[9] H.P. Harding, D. Ron, Endoplasmic reticulum stress and the development of diabetes, Diabetes 51 (Suppl. 3) (2002) S455–S461.

[10] A.A. Osman, M. Saito, C. Makepeace, M.A. Permutt, P. Schlesinger, M. Mueckler, Wolframin expression induces novel ion channel activity in endoplasmic reticulum membranes and increases intracellular calcium, J. Biol. Chem. 278 (2003) 52755–52762.